Building and Environment 261 (2024) 111666

Contents lists available at ScienceDirect

Building and Environment

journal homepage: www.elsevier.com/locate/buildenv

Integration of resilient cooling technologies in building stock: Impact on thermal comfort, final energy consumption, and GHG emissions

Essam Elnagar [a,*], Alessia Arteconi [b,c,d], Per Heiselberg [e], Vincent Lemort [a]

[a] Thermodynamics Laboratory, Aerospace and Mechanical Engineering Department, Faculty of Applied Sciences, Université de Liège, Belgium
[b] Department of Mechanical Engineering, KU Leuven, Leuven, Belgium
[c] EnergyVille, Genk, Belgium
[d] Dipartimento di Ingegneria Industriale e Scienze Matematiche, Università Politecnica Delle Marche, Ancona, Italy
[e] Department of the Built Environment, Aalborg University, Denmark

ARTICLE INFO

Keywords:
Climate change
Cooling systems
Cooling demand
Overheating
Resilience
Building stock

ABSTRACT

Buildings in the EU contribute significantly to energy consumption and greenhouse gas emissions, with HVAC systems being major contributors. This paper assesses the impact of the resilience of various cooling strategies on thermal comfort, energy consumption, and GHG emissions in the residential building stock in Belgium. This study uses an innovative approach for sizing and designing cooling systems, considering the impact of climate change on future weather conditions and extreme heatwaves. The findings reveal alarming temperature increases, with potential rises of up to 4.1 °C from the 2010s to the 2090s, particularly in the high-emission SSP5-8.5 scenario. The study investigates three cooling strategies: scenario 1 (mechanical ventilation), scenario 2 (mechanical ventilation and natural ventilation), and scenario 3 (mechanical ventilation, natural ventilation, and split system). In scenario 1, there is a notable increase in Indoor Overheating Degree (IOhD), reaching up to 586% in the 2090s for semi-detached buildings, while scenario 2 consistently reduces IOhD, reaching only 0.2 °C by the 2090s. Scenario 3 achieves near-zero IOhD by the 2050s and 2090s. Notably, the "Heatwave [2081–2100]" exhibits unprecedented daytime temperatures, peaking at 46.0 °C. During the 2054 heatwave, insulated buildings maintained the Indoor Operative Temperature (IOpT) below 40 °C, whereas non-insulated buildings reached 44.3 °C, indicating challenges in meeting thermal comfort standards. Furthermore, cooling energy consumption increased by 106%–141% in the 2050s and surge by 174%–280% in the 2090s compared to the 2010s, along with significant GHG emissions growth in the future scenarios, particularly in SSP5-8.5.

1. Introduction

1.1. Background

Recent years have witnessed a significant rise in global temperatures and the growing impact of climate change. This elevated consciousness is notably underscored by the Sixth Assessment Report of the Intergovernmental Panel on Climate Change (IPCC), which serves to highlight the imminent imperative of mitigating the repercussions of global warming, with a specific focus on the critical temperature thresholds of 1.5 °C and 2 °C, within the current century. The projections delineated within this report posit the possibility of a discernible escalation in the average global surface air temperature by a range of 1–5.7 °C spanning the period from 2081 to 2100, contextualized in relation to the pre-industrial benchmark between 1850 and 1900 [1,2]. In Europe and Belgium, the rise in temperature is even more pronounced, with increases exceeding the global average due to various local factors [3]. The Paris Agreement emphasizes the need to limit global warming to 1.5 °C above pre-industrial levels. This objective is driven by the understanding that altered precipitation patterns, heatwaves, and rising sea levels pose significant threats. To achieve this, greenhouse gas emissions must peak before 2025 and decline by 43% by 2030. The Paris Agreement aims to strengthen the global response to the climate crisis, emphasizing the importance of collaborative and ambitious actions by nations [4].

Within the European Union (EU), buildings play a substantial role in the energy landscape, accounting for 40% of the total energy consumption and contributing to 36% of its greenhouse gas emissions. This highlights the critical connection between buildings and environmental

* Corresponding author.
E-mail address: essam.elnagar@uliege.be (E. Elnagar).

https://doi.org/10.1016/j.buildenv.2024.111666
Received 1 November 2023; Received in revised form 2 May 2024; Accepted 21 May 2024
Available online 22 May 2024

Nomenclature

A	Opening surface area [m^2]
α	Terrain category parameter [−]
α_{met}	Terrain category parameter at the meteorological station [−]
C_t	Factor representing the effectiveness of the openings [−]
C_w	Opening effectiveness [−]
F	Open area fraction [−]
g	Gravitational acceleration [m/s^2]
ΔH_{NPL}	Difference in height between the middle point of the opening and the neutral pressure point of the building [m]
IOhD	Indoor Overheating Degree hours index [°C]
IndoorTemperatureInfluenceFactor(Q)	Influence factor for cooling capacity [−]
IndoorTemperatureInfluenceFactor(W)	Influence factor for electricity consumption [−]
N_{2012}	Total number of buildings in 2012 [-]
N_{2050}	Total number of buildings in 2050 [-]
$N_{occ}(z)$	Total hours during which a specific zone (z) is occupied [hours]
P_c	Cooling capacity [kW]
PartLoadFactor (T_{out})	Part load factor as a function of outdoor temperature [−]
Q	Total air flow rate [m^3/s]
$Q_{design,c}$	Capacity declared at $T_{design,c}$ [kW]
Q_t	Airflow rate created by temperature difference [m^3/s]
Q_w	Airflow rate created by wind [m^3/s]
Q_{target} (T_{in},T_{out})	Target cooling capacity as a function of indoor and outdoor temperatures [kW]
$T_{design,c}$	Outdoor design temperature [°C]
t	Number of years considered [years]
$t_{i,z}$	Time step [hours]
T_{in}	Indoor temperature inside the building [°C]
$T_{in,z,i}$	Indoor operative temperature in zone (z) at hour (i) [°C]
$TL_{comf,z,i}$	Maximum comfort temperature limits in zone (z) at hour (i) [°C]
T_{out}	Outdoor temperature outside the building [°C]
T_{rm}	Running mean outdoor temperature during the previous seven days [°C]
V_z	Wind speed at the building location [m/s]
V_{met}	Wind speed measured at a meteorological station [m/s]
W_{target} (T_{in},T_{out})	Target electricity consumption as a function of indoor and outdoor temperatures [kW]
X_{con}	Annual construction rate [−]
X_{dem}	Annual demolition rate [−]
Z	Total number of conditioned zones within a building [−]
z	Building zone counter [−]
Z_{met}	Height parameter at the meteorological station [−]
δ	Building's wind boundary layer thickness [m]
δ_{met}	Corresponding parameter at the meteorological station [−]

Abbreviations

ASHRAE	American Society of Heating, Refrigerating, and Air-Conditioning Engineers
BAU	Business-as-usual
CMIP6	Coupled Model Intercomparison Project Phase 6
CO_2	Carbon dioxide
CPENV	Climatic Potential of Extended Natural Ventilation
CPNV	Climatic Potential of Natural Ventilation
DHW	Domestic Hot Water
EER	Energy Efficiency Ratio
ESMs	Earth System Models
EPB	Energy Performance of Buildings Directive
ERA5	Fifth-Generation European Reanalysis
EU	European Union
GHG	Greenhouse Gas
HVAC	Heating, Ventilation, and Air Conditioning
HW	Heatwave
IEA	International Energy Agency
IPCC	Intergovernmental Panel on Climate Change
IOpT	Indoor Operative Temperature
ISO	International Organization for Standardization
km	Kilometre
Kw	Kilowatt
KWh	Kilowatt-hour
MAR	Modèle Atmosphérique Régional (Regional Atmospheric Model)
MM	Mixed-Mode
MV	Mechanical Ventilation
NBN	Bureau for Standardization
NG	Natural Gas
NV	Natural Ventilation
NVP	Natural Ventilation Potential
SAC	Split Air-Conditioned
SET	Standard Effective Temperature
SFP	Specific Fan Power
SPT	Set Point Temperature
TABULA	Typology Approach for Building Stock Energy Assessment
TMY	Typical Meteorological Year

impact, underscoring the urgent need for energy-efficient and sustainable construction practices. The prevalence of buildings in energy consumption is evident not only in the EU but also on a global scale, with buildings globally responsible for 30% of final energy consumption and 26% of energy-related emissions [5,6].

As the world grapples with rising temperatures and increasingly frequent heatwaves, the need for sustainable and resilient cooling technologies in buildings has escalated dramatically. This surge in cooling system usage is driven by the imperative to maintain thermal comfort in the face of extreme heat events caused by climate change [7]. The consequences are twofold: a substantial increase in energy consumption dedicated to cooling and a corresponding rise in GHG emissions, further exacerbating the very climate change that necessitates cooling systems. These interconnected challenges underscore the urgency of addressing cooling technologies and their impact on energy consumption and GHG emissions. A recent study by Elnagar et al. highlights the critical role of innovation in addressing cooling needs while minimizing environmental impacts [8].

1.2. Literature review

The increase in cooling demand is a pressing concern both in different regions of Europe and worldwide. Current studies have shown a notable rise in the demand for cooling, driven by a variety of factors, including climate change, urbanization, income growth, and changing lifestyles. These studies not only reveal the present surge in cooling needs but also project significant increases in the future. Several recent studies have shed light on this trend. For instance, analyses of cooling degree days in various countries have indicated a general increase, leading to higher energy consumption for cooling purposes [9]. European space cooling demands have also been analyzed, revealing disparities between countries and regions [10]. Moreover, projections suggest that by 2050, there will be a substantial increase in cooling energy demand across European Union countries [11]. In 2022, there

was a more than 5% increase in energy consumption for space cooling compared to 2021, continuing the trend of rising demand. Since 2000, the energy demand for space cooling has been steadily increasing, with an average annual growth rate of approximately 4% [6].

The integration of resilient cooling technologies in building stock underscores the critical role of innovation in addressing cooling needs while minimizing environmental impacts. They encompass a wide range of approaches, from passive design measures to active cooling technologies. Current building and building-related system designs have heavily emphasized energy efficiency to mitigate climate change by reducing carbon emissions. However, the rising global temperatures and more frequent heatwaves have underscored the need for strategies that not only optimize energy use but also enhance the resilience of cooling systems in buildings [12,13]. This literature review explores the multifaceted realm of resilient cooling strategies for buildings, with a specific focus on how these strategies can protect against the adverse effects of heatwaves and climate disruptions. Various studies indicated that effective policies have the potential to double the average air conditioning (AC) efficiency, thereby significantly reducing cooling energy demand. Such measures could lead to a remarkable 45% decrease in final energy consumption for cooling compared to reference scenarios [14]. This literature review section explores the current state of cooling strategies, their implications, and potential pathways for addressing the rising demand for cooling in Europe and globally. Traditional cooling methods, including air conditioning systems, have long been the primary means of achieving thermal comfort. However, an evident shift is underway towards sustainable and energy-efficient cooling solutions. Passive cooling systems, natural ventilation, and innovative technologies are gaining prominence as efforts intensify to reduce energy consumption and greenhouse gas emissions [15]. This section delves into two key categories of resilient cooling technologies: passive cooling techniques and active cooling systems. Passive strategies harness natural processes and building design to reduce indoor temperatures without the need for energy-intensive mechanical systems. On the other hand, active systems employ advanced technologies to regulate indoor climates efficiently. Specifically, we will explore the potential of passive cooling techniques like ventilative cooling and the opportunities presented by active systems such as reversible air-to-air heat pumps (split systems).

1.2.1. The role of passive cooling

Passive cooling, with a specific focus on natural ventilation, plays a pivotal role in addressing climate change and curbing the rising cooling demand in buildings. Natural ventilation stands out as a cost-effective and environmentally friendly approach that can significantly reduce the energy consumption associated with cooling in buildings while mitigating the environmental impacts of climate change. Numerous studies have underscored the effectiveness of natural ventilation in achieving these goals. For instance, a review of conventional passive cooling methods highlighted how passive cooling measures, including natural ventilation, can lead to reductions in peak energy demand, minimize temperature fluctuations indoors, and maintain indoor air quality, thus contributing to energy savings and reduced carbon emissions [16]. Additionally, research has shown that natural ventilation combined with controlled shading can have a substantial impact on reducing the cooling energy demand, particularly in hot climate areas, where cooling demand is often highest [17]. This synergy between natural ventilation and other passive cooling techniques is essential in addressing climate change challenges while ensuring indoor comfort and sustainability. Another study by Rodrigues et al. [18] analyzed the impact of natural ventilation on a dwelling in a Mediterranean climate and found that it significantly influenced thermal conditions, contributing to reduced energy consumption. The study found that sizing permanent openings in accordance with standard recommendations demonstrated sufficient performance in delivering anticipated ventilation rates on an average basis. Moreover, Attia et al. [19] focused their attention on a nearly zero-energy building in Belgium. Their research demonstrated that natural ventilation played a pivotal role in preserving thermal comfort within the building, even when confronted with the challenges posed by climate change. This underscores the resilience and adaptability of natural ventilation strategies in maintaining occupant comfort in the face of evolving environmental conditions. In addition to these findings, Elnagar et al. [20] conducted a comprehensive exploration of the application of natural ventilation in Belgium. The study highlighted the capacity of natural ventilation to effectively reduce internal cooling loads during the summer months, presenting a compelling case for its ability to decrease the reliance on active cooling systems. The findings indicated that in the absence of natural ventilation, occupants experience thermal comfort approximately 53.7% of the time. Single-sided ventilation improves this to 66.2%, and cross-ventilation further enhances it to 78.8%. However, during heatwaves, natural ventilation loses its efficiency, and occupants can only achieve thermal comfort 51% of the time under such extreme conditions. Another recent study by Bamdad et al. [21] investigated how natural ventilation strategies may perform in the face of future climate changes. The study introduced two key concepts: the Climatic Potential of Natural Ventilation (CPNV) and the Climatic Potential of Extended Natural Ventilation (CPENV). CPNV quantifies the effectiveness of natural ventilation under current climatic conditions, while CPENV extends the capabilities of natural ventilation by considering elevated airspeed requirements. Studies have shown that this impact is influenced by various factors, including climate and areas. A study by Xie et al. [22] indicated that the potential for natural ventilation (NVP) and cooling energy savings differ significantly between urban and rural areas and are dependent on climate and season. During the summer season, urban areas tend to have lower NVP and cooling energy savings compared to rural areas. These findings emphasize the importance of considering building density and climate conditions when designing and planning for natural ventilation strategies in Chinese regions. Additionally, previous studies, such as one by Tong et al. [23], highlighted the energy-saving potential of natural ventilation. It was found that up to 78% of cooling energy consumption could potentially be reduced through natural ventilation, depending on local weather conditions and air quality.

1.2.2. The role of active cooling

While passive cooling strategies and energy-efficient building designs are promoted to reduce energy consumption and environmental impact, the role of active cooling systems remains essential during peak cooling demand periods. Striking a balance between sustainability and the need for active cooling systems is crucial for ensuring the comfort, health, and safety of occupants in residential buildings, especially during specific challenging times and conditions. Active cooling systems play a crucial role in ensuring comfort and maintaining a habitable environment within residential buildings, especially during specific times and under certain conditions [13]. In regions with extremely high temperatures or periods of heatwaves, active cooling systems become a necessity to protect occupants from heat-related health risks and to maintain productivity and well-being. These systems are particularly important in densely populated urban areas where heat buildup can be exacerbated by the urban heat island effect. Additionally, active cooling systems can be vital in providing thermal comfort for vulnerable populations, including the elderly, young children, and individuals with certain medical conditions [7,24]. Several studies highlighted the importance of implementing effective cooling strategies as a crucial response to mitigate the challenges of overheating caused by climate change [25–27]. A review study by Bandyopadhyay et al. [28] discussed the existing space cooling technologies and their suitability for providing comfort cooling, particularly in warm and humid climates. The study highlighted the importance of efficient cooling systems in addressing environmental concerns. Additionally, a recent study by Yan et al. [29] investigated the impact of setting a minimum cooling set point temperature (SPT) of 26 °C in office buildings. The findings indicated

that 45% of the air conditioner SPTs were below 26 °C. In the high SPT mode (SPT≥26 °C), people exhibited better physiological adaptation to the warmer environment and were more likely to adjust by wearing lighter clothing and increasing air velocity to improve thermal discomfort. However, when comparing the two SPT modes within the same Standard Effective Temperature (SET) ranges, no significant differences were observed in thermal sensation, acceptability, or comfort. SET is a measure used to evaluate thermal comfort in indoor environments. It considers factors such as air temperature, humidity, air velocity, and mean radiant temperature to provide a comprehensive assessment of the overall thermal environment experienced by individuals. Another study by Yan et al. [30] investigated split air-conditioned (SAC) buildings in China employing manual changeover mixed-mode (MM) during the summer, which combines air-conditioned (AC) and natural ventilation (NV) modes. The findings revealed that occupants in AC mode experienced cooler thermal conditions with an acceptable temperature limit of around 30 °C compared to those in NV mode. These findings provide valuable insights into the dynamics of thermal comfort in SAC buildings, guiding the application of adaptive models and setting temperature limits for occupant comfort under varying outdoor conditions.

In addition to the aforementioned studies, additional studies can be found at the building scale [24,31–37] and building stock scale [25,38–41], as detailed in Table 1. This table comprises various studies investigating the impacts of climate change on different aspects of European buildings, including thermal comfort, heating and cooling demands, and GHG emissions. These studies utilize a range of approaches, including typical, representative, or hybrid approaches, as explained in detail in section 2.2.

1.3. Knowledge gap

While numerous studies have investigated the influence of climate change on energy demand at the individual building level [24,31–37], there is a notable limit of research at the broader building stock scale, especially when adopting a multi-zone approach at that scale [25,38–41]. Current research often focuses on small clusters, failing to capture the interconnected dynamics and systemic effects across diverse building types and environments [19,24]. Moreover, comprehensive research that encompasses all aspects of time-integrated discomfort, energy use for cooling systems, and GHG emissions remains relatively limited. Many of these studies lack a thorough assessment of time-integrated discomfort with high-resolution climate data. Furthermore, it is worth noting that most of these studies make certain assumptions about the type of cooling system without providing detailed information on their modelling procedures or the sizing systems used under future climate conditions. Notably, a significant gap exists as most of the previous studies often neglect changes in the sizing of cooling systems required to address the evolving cooling demands arising from climate change and during heatwaves. This underscores the need for research and a dedicated study that specifically examines the impact of integrating resilient cooling technologies into building stocks, considering a climate change-sensitive sizing and design approach.

1.4. Paper contribution

The primary contribution of this study is the comprehensive assessment of the impact of integrating various resilient cooling technologies into the building stock in Belgium. This assessment encompasses thermal comfort, energy consumption, and greenhouse gas emissions across different building types, evaluated through different key performance indicators (KPIs). The study takes into account various weather scenarios, including Typical Meteorological Years (TMYs) and specific historical, mid-future, and long-future heatwaves. This comprehensive approach allows for a thorough examination of the performance of active cooling systems under different climatic conditions, ensuring a robust understanding of their effectiveness in mitigating heat-related challenges. Crucially, this paper delves into the climate change-sensitive sizing of active cooling systems, guided by ISO 15927–2, across these diverse weather scenarios. By integrating climate change considerations into the sizing process, the study acknowledges the evolving nature of climate conditions and the necessity for adaptive design strategies to maintain thermal comfort standards amidst changing environmental dynamics. This addresses a critical aspect often overlooked in previous studies, as this paper also evaluates whether the sizing guidelines are effective in meeting thermal comfort standards

Table 1
Summary of the recent studies on the impact of climate change on thermal comfort, heating demand, cooling demand, and GHG emissions in European buildings.

Study	Location	Year	Building			Study focus
			Type	Scale	Approach	
Olonscheck et al. [38]	Germany	2012	Residential	Building stock	Representative	Heating demand, cooling demand, and GHG emissions
Roetzel and Tsangrassoulis [31]	Greece	2012	Commercial	Building scale	Typical	Heating demand, cooling demand, thermal comfort, and GHG emissions
Nik and Kalagasidis [39]	Sweden	2013	Residential	Building stock	Typical	Heating demand and cooling demand
Berger et al. [32]	Austria	2014	Commercial	Building scale	Representative	Heating demand and cooling demand
Jylhä et al. [33]	Finland	2015	Residential	Building scale	Typical	Heating demand and cooling demand
Van Hooff et el [34].	Netherlands	2016	Residential	Building scale	Typical	Heating demand and cooling demand
Hamdy et al. [40]	Netherlands	2017	Residential	Building stock	Typical	Thermal comfort
Pérez-Andreu et al. [35]	Spain	2018	Residential	Building scale	Typical	Heating demand, cooling demand, and thermal comfort
Moazami et al. [36]	Switzerland	2019	Residential and commercial	Building scale	Representative	Heating demand and cooling demand
Larsen et al. [41]	Europe	2020	Residential and commercial	Building stock	Representative	Heating demand and cooling demand
De Masi et al. [37]	Italy	2021	Residential	Building scale	Representative	Heating demand and cooling demand
Rahif et al. [24]	Belgium	2022	Residential	Building scale	Typical	Heating demand, cooling demand, thermal comfort, and GHG emissions
Elnagar et al. [25]	Belgium	2023	Residential	Building sock	Hybrid	Heating demand and cooling demand

during heatwaves. Furthermore, this paper provides a valuable contribution by offering a simple polynomial model for all the cooling systems assessed in this study. This model aids in understanding the performance and impact of these systems, contributing to the broader body of knowledge on resilient cooling technologies in the face of climate change. By providing a standardized framework for evaluating cooling system performance, the study contributes to advancing the understanding and adoption of resilient cooling technologies, thereby promoting the development of more sustainable and climate-resilient building stocks. The findings and insights from this study are instrumental for policymakers, building designers, and engineers working to enhance the resilience and sustainability of building stocks in a changing climate.

The paper is structured as follows: Section 2 outlines the methodology, including the conceptual framework (Section 2.1), building stock scenarios (Section 2.2), climate data (Section 2.3), key performance indicators (Section 2.4), cooling strategies (Section 2.5), and climate-sensitive sizing (Section 2.6). Section 3 presents the results, and Section 4 discusses key findings, strengths, limitations, and future research directions. Finally, Section 5 concludes the paper.

2. Methodology

2.1. Conceptual framework

In this study, the conceptual framework serves as the roadmap for conducting a comprehensive analysis of the impact of different cooling strategies within the building stock on thermal comfort, energy consumption, and greenhouse gas emissions, as shown in Fig. 1.

The first phase involves the selection of a reference city and climate data. Brussels is chosen as the reference city, and its climate data are categorized into two main parts: TMY and heatwaves weather data, encompassing various SSPs. The second phase of the framework is centred around building stock scenarios. For this study, the focus is on cooling systems scenarios. Specifically, different cooling strategies are applied to the entire building stock. Following this, the study progresses to specifying the fixed and dynamic parameters required for the calculation of cooling energy demand. The third phase revolves around the identification of the three distinct cooling strategies employed in this research: Strategy 1 involves mechanical ventilation, Strategy 2 combines mechanical ventilation with natural ventilation, and Strategy 3 integrates mechanical ventilation, natural ventilation, and split systems for active cooling. Subsequently, the study enters the results phase, where key performance indicators (KPIs) are employed to assess thermal discomfort, energy consumption, and GHG emissions associated with these cooling strategies. The following KPIs are suggested for cooling technology performance assessment, selected from the International Energy Agency (IEA) EBC Annex 80 – 'Resilient cooling of buildings' project. These KPIs evaluate the performance of the cooling systems, covering all essential aspects necessary for assessment. These KPIs are essential for understanding occupant comfort, energy efficiency, and environmental sustainability. While these KPIs form a solid foundation for comprehensive research on cooling systems, It might be necessary to incorporate additional metrics depending on their specific objectives and context. The final stages of the framework encompass the simulation engine, the simulation process, and post-processing activities. These are

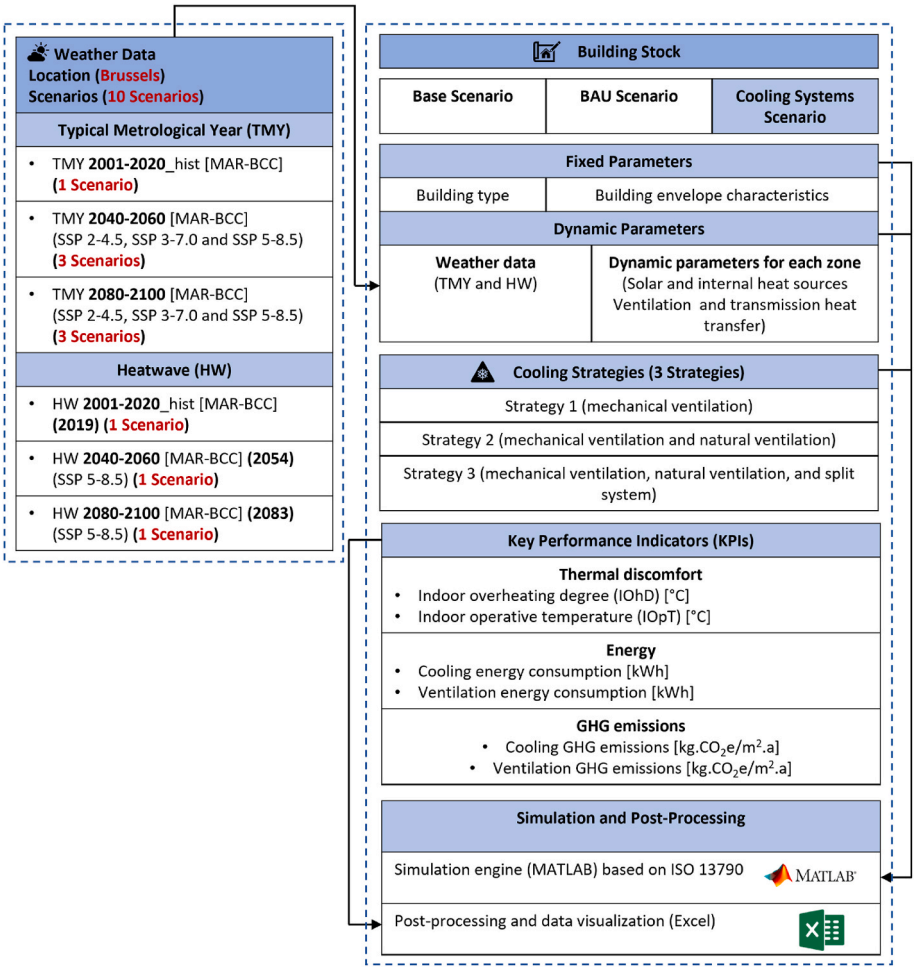

Fig. 1. Conceptual framework of the study.

critical for analyzing and visualizing the data generated throughout the study, ensuring a robust evaluation of the different cooling strategies' impact on building stock in a changing climate.

2.2. Building stock model

In this study, we have used a comprehensive tree structure model that was developed as part of our previous study by Elnagar et al. [25] to represent the residential building stock in Belgium within our research framework. This tree structure serves as a tool for assessing the impact of various HVAC technology adoption scenarios on national-level electricity and gas load profiles [42] and the annual energy consumption of the entire building stock [43]. The architecture of the tree structure is shown in Fig. 2, where three scenarios are considered: the base scenario, the Business as Usual (BAU) scenario, and the cooling systems scenario.

In this study, a "hybrid approach" is used, which combines elements from both the "typical approach" and the "representative approach" in building stock typology, as described by Cyx et al. [44]. The "representative approach" models fictional buildings with average characteristics, adjusted to match overall energy consumption patterns. Conversely, the "typical approach" extends a standard building's attributes to closely resemble real-world structures [44–46]. This hybrid approach bridges the gap between the broader overview of the representative approach and the detailed insights of the typical approach, yielding a comprehensive understanding of the building stock and its energy utilization, encompassing both aggregate and specific building types.

The creation of a comprehensive building stock tree structure is a complex task involving the consideration of various scenarios and assumptions. Initially, an exhaustive examination of all potential cases based on available statistics is necessary. This process results in a substantial number of cases, each of which requires more than two days of computation to simulate just one possible scenario. Consequently, simplifications are introduced to manage this computational complexity. The methodology developed to create the tree structure is described in detail in the previous study by Elnagar et al. [25] and in another study by Gendebien et al. [47]. To encompass the various building typologies and age categories, the geometric attributes of 16 prototypical buildings are expanded to encompass a broader array of buildings. These 16 typical buildings are representative of four building types (freestanding, semi-detached, terraced, and apartments) and encompass five distinct construction periods within the base scenario (pre-1945, 1946–1970, 1971–1990, 1991–2007, and 2008–2012), and additional construction period (2013–2050) in the BAU scenario and cooling systems scenario, as shown in Fig. 2. The same building geometry reference is applied to both the 1991–2007 and 2008–2012 construction periods.

Within each construction period and associated building geometry, the tree structure model further distinguishes the three aforementioned scenarios, considering factors such as insulation levels. A visual representation of the distribution of average U-values for both walls and windows in the building stock in the base scenario is shown in Fig. 3. The choice of energy source for space heating and domestic hot water (DHW) and the selection between centralized heating production systems (e.g., boilers) and decentralized heating production systems (e.g., electric resistive heaters and gas convectors).

The final configuration of the building stock tree structure is developed by taking into account six key parameters.

1. Building type: this parameter classifies buildings into distinct categories, including freestanding, semi-detached, terraced, and apartments.
2. Year of construction: buildings are categorized based on the time periods in which they were constructed, including pre-1945, 1946–1970, 1971–1990, 1991–2007, 2008–2012, and 2013–2050 (for the BAU scenario and cooling systems scenario).
3. Insulation level: this parameter characterizes the degree of insulation within the building envelope, encompassing walls, windows, roofs, and floors.
4. Space heating energy vectors: This parameter shows the energy sources employed for space heating, including fuel, natural gas (NG), electricity, and alternative options such as coal or wood.
5. Heating production system: This parameter distinguishes between centralized and decentralized heating systems.
6. DHW energy vectors: This parameter represents the energy sources utilized for domestic hot water (DHW), encompassing fuel, NG, electricity, and alternative sources like coal or wood.

2.2.1. Base scenario

The base scenario is divided into 752 distinct cases, collectively representing a substantial building stock of 4,675,433 structures. Among these cases, 202 are devoted to each of the freestanding, semi-

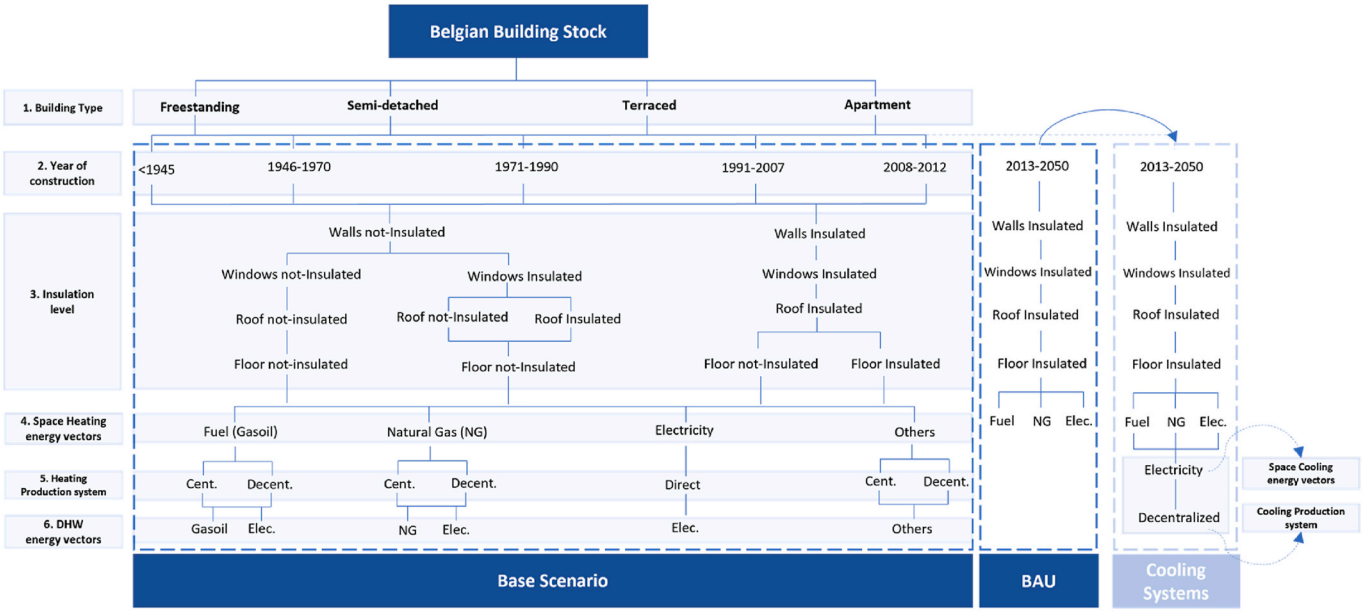

Fig. 2. Tree structure model of the Belgian residential building stock.

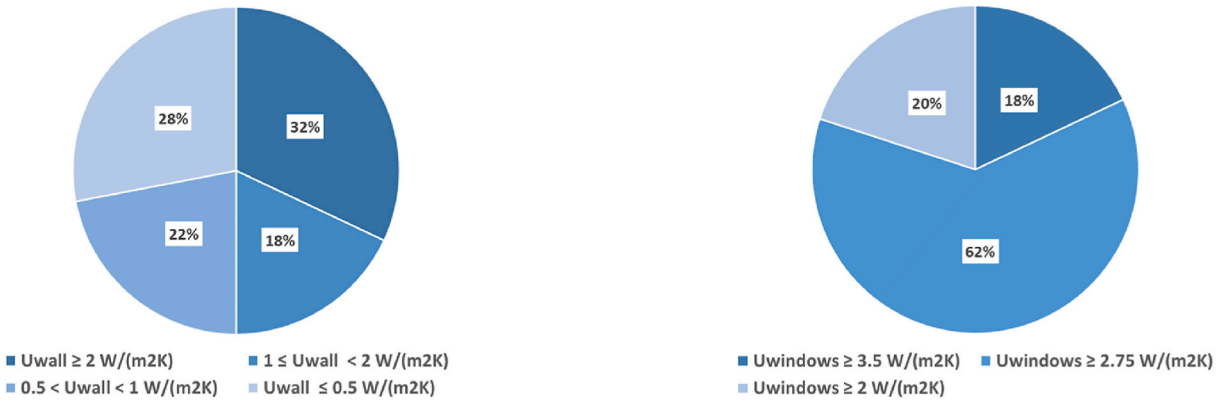

Fig. 3. U-values repartition for walls and windows.

detached, and terraced housing categories, while apartments comprise 146 cases. The distribution of the Belgian dwelling types by the five construction periods for the base scenario is shown in Fig. 4 (a). This base scenario primarily focuses on investigating the dynamics of heating and cooling energy demands in the context of climate change, with specific attention to the building stock. Notably, this examination does not encompass any demolition or renovation strategies.

2.2.2. BAU scenario

The BAU scenario involves the projection of the building stock up to the year 2050. To accomplish this, the existing tree structure representing the building stock as of 2012 is transformed into an evolutionary tree structure, enabling simulations to explore potential changes within the building stock over time. This transformation incorporates annual rates for demolition, construction, deep retrofit, and shallow retrofit. Initially, the tree structure is updated to account for newly constructed and demolished buildings spanning the period from 2013 to 2050. In alignment with the long-term renovation strategies adopted in Brussels, Wallonia, and Flanders regions of Belgium, the average annual construction and demolition rates are set at 0.9% [48–51] and 0.075% [52], respectively. The total number of buildings projected for the year 2050 is calculated using equation (1):

$$N_{2050} = N_{2012}(1 + (x_{con} - x_{dem}))^t \quad (1)$$

With.

- N_{2012}: total number of buildings in 2012
- N_{2050}: the total number of buildings in 2050
- X_{con}: annual construction rate;
- X_{dem}: annual demolition rate;
- t: number of years considered (i.e. t = 38 years).

This scenario explores two renovation strategies: deep renovation, which involves extensive insulation upgrades for all building components, and shallow renovation, primarily focusing on roof and window insulation according to the EPB Directive 2010 [53]. Priority was given to deep renovation for the oldest non-insulated buildings, followed by shallow renovation for partially insulated ones. These strategies aim to enhance energy efficiency and indoor comfort. In this scenario, the number of dwellings will reach 6,152,311 by 2050. The distribution of the Belgian dwelling types by the six construction periods for the BAU scenario is shown in Fig. 4 (b).

In our previous study by Elnagar et al. [25], uncertain scenarios were addressed surrounding future renovation rates, which can be influenced by factors like regulations, consumer behaviour, and funding availability. Uncertainty analysis was conducted involving eight renovation scenarios, each with different demolition, shallow renovation, and deep renovation rates. These scenarios explored the potential impact of uncertain renovation rates on heating and cooling energy demands.

Table A. 1 and Table A. 2 in Appendix A show more details and the parameters used for modelling to obtain a more detailed understanding of the building stock.

2.2.3. Cooling systems scenario

The cooling systems scenario, one of the new HVAC scenarios presented in our study, complements the previous scenarios involving electricity-driven heat pumps and gas-driven heat pumps, as detailed in our prior study by Elnagar et al. [54].

In this cooling systems scenario, various resilient cooling systems are integrated into the building stock. These systems encompass passive cooling methods, such as ventilative cooling facilitated by mechanical and natural ventilation, along with active cooling systems, specifically the split air-conditioning system (reversible air-to-air heat pump). It's important to note that this scenario builds upon the same tree-structure model utilized in the BAU scenario, with the incorporation of these

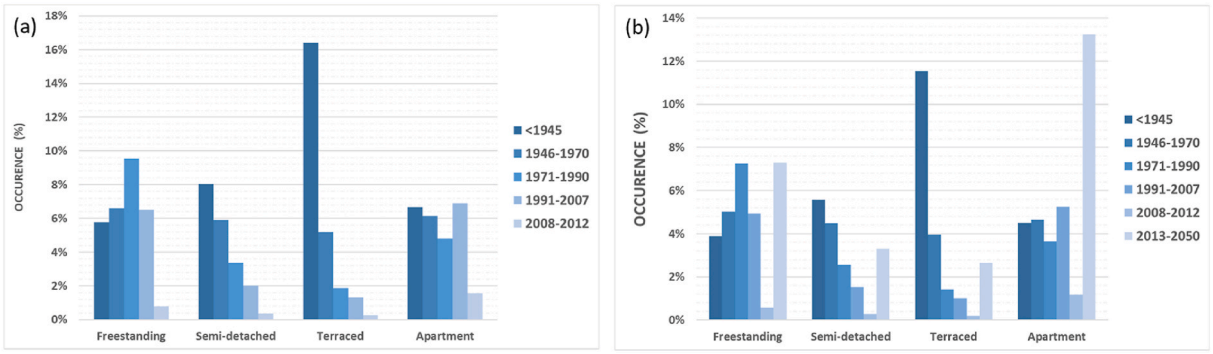

Fig. 4. Distribution of the Belgian dwelling types by the different construction periods (a) base scenario (b) BAU scenario.

resilient cooling systems into the building stock.

In this scenario, it is assumed that all buildings are equipped with mechanical ventilation systems and split air-conditioning systems. Moreover, natural ventilation is implemented across the entire building stock. By incorporating these assumptions into the scenario, the potential impact of such comprehensive cooling systems on the overall energy consumption and thermal comfort of the building stock is evaluated. This scenario aims to assess the effectiveness of these systems in mitigating the effects of climate change and enhancing building resilience.

2.3. Climate data

This study uses the "Modèle Atmosphérique Régional" model, denoted as "MAR" version 3.11.4 [55]. The primary objective of MAR is to refine the spatial and temporal resolution of weather data by downscaling a global model or reanalysis, achieving resolutions of approximately 100 km every 6 h and 30 km every 3 h, respectively, to attain finer weather outputs, typically at a 5 km resolution every 1 h. Several studies have validated this model for the Belgian territory [56–59]. In this study, the MAR model operates at a spatial resolution of 5 km.

Like any regional climate model, the MAR model relies on boundary conditions provided by a global model, such as an Earth System Model (ESM) or a reanalysis model. In the past simulation phase (1980–2020), the MAR model was forced by ERA5, referred to as MAR-ERA5 [60]. Since ERA5 relies on various observation sources (e.g., in-situ weather stations, radar data, satellites, etc.), MAR-ERA5 can be considered the simulation that most closely approximates observed climate conditions. In the second phase, the MAR model is driven by three Earth System Models (ESM) selected from the Sixth Coupled Model Intercomparison Project (CMIP6 [2]). These selections are based on two criteria: their representation of atmospheric circulation over Western Europe relative to ERA5 during the period 1980–2014 and their alignment with the CMIP6 models' projected scenarios for 2100 under the SSP5-8.5 scenario [55]. The chosen ESMs for this study is BCC-CSM2-MR (MAR-BCC) [61].

It's important to note that these ESMs do not depend on observations and solely depict the mean evolution of climate under various carbon emissions scenarios, corresponding to distinct Shared Socioeconomic Pathways (SSPs) [62]. Except for MAR-MIR, which exhibits a noticeable overestimation of summertime temperatures and solar radiation, the MAR simulations effectively capture current climate conditions and their year-to-year variability. The ensemble mean of all MAR simulations is MAR-BCC, while MAR-MPI is characterized as the coldest of the MAR simulations. Initially, the ESMs force MAR in accordance with their historical scenario (1980–2014) to facilitate a comparative analysis with MAR-ERA5. Subsequently, the ESMs are utilized to drive MAR under the most warming scenario, SSP5-8.5, to project future climate changes (2015–2100).

The SSP5-8.5 scenario is employed to reconstruct the SSP3-7.0 and SSP2-4.5 scenarios to save computational time. This reconstruction is based on the fact that the climate evolution in SSP5-8.5 encompasses the evolution in SSP3-7.0 and SSP2-4, as explained by Doutreloup et al. [55].

In the first part of this study, Typical Meteorological Year (TMY) datasets are used. TMY datasets, which provide synthetic hourly data, are created by selecting representative months based on the distribution of each month within a long-term dataset (minimum ten years) using Finkelstein-Schafer statistics [63]. Various methods exist for generating TMY datasets [64], but this study employs a protocol developed in accordance with ISO15927-4 [65], as detailed in Doutreloup et al. [55].

In addition to using the TMY datasets, this paper investigates the effectiveness of different cooling strategies during summer heatwaves. In Belgium, two distinct definitions of heatwaves are employed. The retrospective heatwave is defined in accordance with the criteria set forth by the Royal Meteorological Institute, necessitating a continuous 5-day span with daily maximum temperatures of 25 °C or above (referred to as summer days) and an additional requirement of a 3-day period where temperatures reach 30 °C or higher [66]. Conversely, the prospective heatwave is characterized by a continuous 3-day duration with minimum temperatures averaging 18.2 °C or higher across the three days, coupled with maximum temperatures reaching 29.6 °C or higher [67]. The provided definition in Belgium does not account for regional climate variations. Furthermore, the use of a fixed threshold for defining heatwaves can introduce distortions when comparing data obtained from various ESMs, given that each ESM has its own unique values and variations.

In contrast, this study adopted an alternative definition of heatwaves, taking into account the local climate characteristics of each region. This definition draws from the statistical framework proposed by Ouzeau et al. [68], which categorizes heatwave events and classifies them based on three key criteria: their duration (number of consecutive days during the heatwave period), maximal temperature (the maximum recorded daily mean temperature), and their overall intensity (the cumulative difference between the outdoor temperature and the temperature threshold (S_{deb}) for the whole duration of the event, divided by the difference between S_{deb} and S_{pic}). S_{deb} and S_{pic} represent the 97.5% and 99.5% percentiles of the air temperature dataset for the reference period. This study focuses on identifying heatwaves with the highest maximum temperatures during three distinct time frames: 2001–2020 (representing the historical scenario), 2041–2060 (reflecting the mid-future scenario), and 2081–2100 (projecting the future scenario). These time periods align with those used for the TMY datasets.

The choice of these specific time periods adheres to the guidance outlined in the dynamic simulation guideline by the IEA EBC Annex 80 – 'Resilient cooling of buildings' project, as detailed in Ref. [69].

2.4. Key performance indicators

In the study mentioned, a comprehensive evaluation of climate change impact and the integration of resilient cooling strategies is achieved. Two main categories of Key Performance Indicators (KPIs) are used. The assessment extends beyond the quantification of final cooling energy consumption as it delves into GHG emissions and thermal comfort.

2.4.1. Time-integrated thermal discomfort

In the context of assessing thermal comfort, particularly in the evaluation of overheating in buildings, time-integrated thermal discomfort indicators play a key role. These indicators can be classified as symmetric, addressing both overheating and overcooling, or asymmetric, focusing solely on one of these aspects. In this study, an asymmetric indicator known as the Indoor Overheating Degree (IOhD) is selected to evaluate overheating discomfort [40,70]. The IohD index is derived by aggregating heating degree hours over the total number of zonal occupied hours. The formula for calculating IohD is as follows in equation (2):

$$IOhD = \frac{\sum_{z=1}^{Z}\sum_{i=1}^{Nocc(z)}\left[\left|T_{in,z,i-TL_{comf,z,i}}\right|\right].t_{i,z}}{\sum_{z=1}^{Z}\sum_{i=1}^{Nocc(z)}t_{i,z}}\ [^{\circ}C] \quad (2)$$

With (z) represents the building zone counter, (Z) signifies the total number of conditioned zones within a building, (i) is the occupied hour counter, and ($N_{occ(z)}$) denotes the total hours during which a specific zone (z) is occupied. Furthermore, ($T_{in,z,i}$) signifies the indoor operative temperature in a zone (z) at the specific hour (i) when no heating or cooling systems are operating, while ($TL_{comf,z,i}$) corresponds to the maximum comfort temperature limits in a zone (z) at the same hour (i). The variable (t) represents the time step, typically set at 1 h. Notably, the summation process considers only positive differences between ($T_{in,z,i}$) and ($TL_{comf,z,i}$).

The $TL_{comf,z,i}$ is derived through reference to established static or adaptive comfort models (adaptive or static) in recognized standards such as ISO 17772 [71] and EN 16798 [72].

Overall, the IohD is a multi-zonal approach that evaluates both the intensity and frequency of indoor overheating events in a building with a single value. The intensity is evaluated by measuring the temperature difference between indoor operative temperature ($T_{in,z,i}$) and the chosen maximum comfort temperature limit ($TL_{comf,z,i}$). Meanwhile, the frequency of overheating is calculated by integrating the intensity of overheating occurrences during the occupied period (N_{occ}) across different building zones (z), allowing for a comprehensive assessment of the overall overheating situation within the building.

In this paper, two distinct thermal comfort models have been used to address varying cooling strategies within the context of building environments. The first model is the adaptive thermal comfort model which adheres to ISO 17772 guidelines [71]. It is used for scenarios in which buildings rely solely on natural ventilation systems during occupied hours without the utilization of active cooling systems. Within this adaptive comfort model, the ($TL_{comf,z,i}$) is calculated as shown in equation (3):

$$TL_{comf,z,i} = 0.33\ T_{rm} + 21.8 \tag{3}$$

Where T_{rm} is the running mean outdoor temperature during the previous seven days. Conversely, when dealing with cooling strategies that involve actively cooled building zones, a static comfort model is employed. In this configuration, the maximum comfort temperature limit ($TL_{comf,z,i}$) is set at 26 °C. This particular temperature threshold serves as a fixed reference point in the static comfort model, offering a distinct approach to thermal comfort assessment in contrast to the adaptive model. Overall, the adaptive model accommodates natural ventilation systems, and the static model provides a benchmark for actively cooled zones.

2.4.2. Final energy consumption and GHG emissions

The focus extends beyond assessing the impact of climate change on thermal comfort in Belgian households; it also assesses the aspects of energy consumption and GHG emissions. Given the integration of electricity-driven cooling strategies in the context of variable weather scenarios, it is important to understand the impact on final cooling energy consumption and associated GHG emissions. This analysis provides insights into how the utilization of these cooling strategies affects the overall energy demand in different climatic conditions. Additionally, the study quantifies the GHG emissions resulting from final energy consumption by employing a CO_2 conversion factor for electricity, calculated at 0.161 kg. CO_{2e}/kWh for Belgium [73,74].

2.5. Application of resilient cooling strategies

2.5.1. Passive cooling strategies

In the realm of modern building design, effective cooling and ventilation strategies are essential to create comfortable and healthy indoor environments. Among these strategies, mechanical ventilation stands out as a versatile and energy-efficient method. This section explains the application of mechanical ventilation as the first cooling scenario applied to the entire building stock. Mechanical ventilation serves the dual purpose of maintaining Indoor air quality and controlling indoor temperatures through fans to facilitate the inflow of fresh outdoor air through ducts. Its cooling function is initiated under specific conditions, necessitating that the indoor temperature exceeds a predefined set-point (in this study, the cooling set point is defined at 26 °C) while the outdoor air temperature is at least two degrees cooler than the indoor air temperature.

The ventilation rates in mechanical ventilation system design are essential to ensure compliance with indoor air quality standards while optimizing energy efficiency. Guided by the NBN D 50-001 standard, which considers factors like occupancy, floor area, and outdoor air requirements, strict adherence guarantees that the mechanical ventilation rate for each zone aligns with the minimum requirements. Specific rates are prescribed for different zones, including sleeping rooms at 25 m^3/h, kitchen and bathroom at 50 m^3/h, and the living room at 75 m^3/h. Specific Fan Power (SFP) values are typically considered as 1.6 W/m^3/s for existing buildings and 1.1 W/m^3/s for new buildings. These values represent the electrical power consumed per unit of airflow by the fan system.

Additionally, this section explores the principles and methodology involved in achieving natural ventilation as the second cooling strategy; unlike mechanical ventilation, which relies on fans, natural ventilation primarily involves opening windows to allow outside air to enter the building. This cooling strategy is contingent on specific conditions, such as the indoor temperature exceeding the set point and the outdoor temperature being at least two degrees cooler. There are twin main factors in our study contributing to natural ventilation.

- **Pressure difference due to wind**

It is crucial to determine the wind speed at the building location. This is achieved through a calculation based on the ASHRAE (American Society of Heating, Refrigerating, and Air-Conditioning Engineers) methodology [75]. The formula used is as follows in equation (4):

$$V_z = V_{met} \cdot \left(\frac{\delta_{met}}{z_{met}}\right)^{\alpha_{met}} \cdot \left(\frac{z}{\delta}\right)^{\alpha} \tag{4}$$

With.

- V_z is the wind speed at the building location [m/s].
- *Vmet* is the wind speed measured at a meteorological station [m/s].
- δ, α, and Z are parameters related to the building's wind boundary layer thickness, terrain category, and height.
- δ_{met}, α_{met}, and Z_{met} are the corresponding parameters at the meteorological station where data is collected.

Once the wind speed is determined, the airflow rate created by wind is calculated by equation (5):

$$Q_w = C_w.A.F.V_z \tag{5}$$

With.

- Q_w is the airflow rate in [m^3/s].
- A is the opening surface area in [m^2].
- F is the open area fraction (ranging from 0 to 1).
- V_z is the wind speed [m/s].
- C_w is the opening effectiveness, calculated as shown in equation (6):

$$C_w = 0.55 - \frac{|window\ direction - wind\ direction|}{180}.\ 0.25 \tag{6}$$

With.

- Window direction is the direction of the window in degrees from the north.
- Wind direction is the direction of the wind in degrees from the north.

- **Temperature difference**

In addition to wind-induced pressure differences, temperature differences between the indoor and outdoor environments also influence natural ventilation. The airflow created by the difference in temperature is driven by equation (7).

$$Q_t = C_t.A.F.\sqrt{2.g.\Delta H_{NPL}.\frac{|T_{in} - T_{out}|}{T_{in}}} \tag{7}$$

With.

- Qt is the airflow rate in cubic meters per second.
- C_t is a factor that represents the effectiveness of the openings, calculated as shown in equation (8).
- A is the opening surface area in square meters.
- F is the open area fraction (ranging from 0 to 1).
- G is the gravitational acceleration at the Earth's surface, equal to 9.81 m/s^2
- ΔH_{NPL} is the difference in height between the middle point of the opening and the neutral pressure point of the building, equal to 0.5.
- T_{in} is the indoor temperature inside the building
- T_{out} is the outdoor temperature outside the building

$$C_t = 0.40 + 0.0045.|T_{in} - T_{out}| \tag{8}$$

Then, the total air flow rate is calculated based on equation (9).

$$Q = \sqrt{Q_w^2 + Q_t^2} \tag{9}$$

2.5.2. Active cooling strategies

Following the exploration of mechanical and natural ventilation as sustainable cooling strategies, the third approach involves active cooling systems utilizing a reversible air-to-air heat pump, commonly known as a split system. This advanced cooling method offers precise temperature control for indoor environments. A split system is comprised of two main components: an indoor unit and an outdoor unit. The indoor unit is installed within the building, while the outdoor unit is placed outside. This cooling system operates by transferring heat from the indoor space to the outdoors during cooling mode and vice versa during heating mode. It achieves this through a refrigeration cycle involving a compressor, condenser, expansion valve, and evaporator. In cooling mode, the system extracts heat from the indoor air and releases it outside, resulting in cooler indoor temperatures. Conversely, in heating mode, it absorbs heat from the outdoor air and brings it inside to maintain warmth [13].

This study incorporates two different split systems and one multi-split system manufactured by Daikin, each characterized by different cooling capacities of 3.5 kW and 9.5 kW for the split systems and 22 kW for the multi-split system. The selection of these split systems was made with consideration aimed at addressing a wide range of building stock typologies to meet the cooling needs of various building types. Table 2 provides the declared cooling capacity (*Pc*) and the manufacturer-supplied Energy Efficiency Ratio (EER) values for the various systems modelled within this study. These values are indicated at different outdoor temperatures and a fixed indoor temperature of 27 °C.

In practice, the manufacturer-declared values are typically provided at a fixed indoor temperature (27 °C). However, to assess the performance of these systems comprehensively, it is essential to consider a range of indoor temperatures. To address this need, we used an established polynomial model, which has been validated through experimental work for another split system. This model takes into account the indoor temperature as a variable when calculating electricity consumption and system capacity. This approach enables us to evaluate system performance under a broader range of operating conditions. Third-degree polynomial equations, as represented by equations (10) and (11), are employed as fundamental mathematical tools for the determination of the cooling capacity (Q) and electricity consumption (W) of the system under varying indoor and outdoor temperature conditions. Additionally, the Gauss-Newton method was used to iteratively determine the values of the parameters ($C1_{capacity}$: $C11_{capacity}$ and $C1_{power}$: $C11_{power}$) that optimize the system's performance to align with the predefined target performance criteria.

$$\begin{aligned} Q_{target}(T_{in}, T_{out}) = {} & C1_{capacity} + C2_{capacity}\, T_{in} + C3_{capacity}\, T_{in}^2 + C4_{capacity}\, T_{in}^3 \\ & + C5_{capacity}\, T_{out} + C6_{capacity}\, T_{out}^2 + C7_{capacity}\, T_{out}^3 \\ & + C8_{capacity}\, T_{in}\, T_{out} + C9_{capacity}\, T_{in}\, T_{out}^2 + C10_{capacity}\, T_{in}^2 T_{out} \\ & + C11_{capacity}\, T_{in}^2\, T_{out}^2 \end{aligned} \tag{10}$$

$$\begin{aligned} W_{target}(T_{in}, T_{out}) = {} & C1_{power} + C2_{power}\, T_{in} + C3_{power}\, T_{in}^2 + C4_{power}\, T_{in}^3 \\ & + C5_{power}\, T_{out} + C6_{power}\, T_{out}^2 + C7_{power}\, T_{out}^3 \\ & + C8_{power}\, T_{in}\, T_{out} + C9_{power} T_{in}\, T_{out}^2 + C10_{power} T_{in}^2 T_{out} \\ & + C11_{power} T_{in}^2\, T_{out}^2 \end{aligned} \tag{11}$$

Initially, the declared system performance, referred to as 'target values', is explicitly defined based on the manufacturer's provided data. Notably, for parameters such as EER and cooling capacity, only four target values are available from the manufacturer, as shown in Table 2. Given that the experimental data for a different system characterized by a lower capacity was assessed earlier, a performance curve for such a system has been evaluated. In this new model, to align the performance characteristics of the new systems with this existing curve, we have introduced a novel parameter termed the 'Indoor Temperature Influence Factor'. This factor is calculated as described in equation (12). It is used to calculate the target cooling capacities for varying indoor temperatures. The factor assumes a value of 1 when the indoor temperature is maintained at 27 °C. However, it progressively decreases as the indoor temperature exceeds 27 °C and conversely increases when the indoor temperature falls below 27 °C. Therefore, the target capacities are defined based on equation (13) using the part load factor, which is calculated as shown in equation (14).

$$IndoorTemperatureInfluenceFactor\ (Q) = 1 - \frac{(T_{in} - T_{in-partload}).(T_{out} - 3) * 0.066}{100} \tag{12}$$

$$Q_{target}(T_{in}, T_{out}) = \frac{Q_{designc}.PartLoadFactor(T_{out})}{IndoorTemperatureinfluencefactor(Q)(T_{in})} \tag{13}$$

$$PartLoadFactor(T_{out}) = \frac{T_{out} - 16}{T_{design,c} - 16} \tag{14}$$

With.

- $T_{design,c}$ is the outdoor design temperature, which equals 35 °C
- $Q_{design,c}$ is the capacity declared at $T_{design,c}$

The same concept is employed to determine the values of the parameters required for calculating target values of electricity consumption while considering that the EER is calculated as shown in equation (15). Therefore, the target value of the electricity consumption is calculated based on equation (16). Indoor Temperature Influence Factor (Q) and Indoor Temperature Influence Factor (W) have been manually developed to incorporate the influence of indoor temperature on capacity and power consumption within an existing model. While these

Table 2
Cooling capacity and EER values for the different split and multi-split systems declared by the manufacturer at a fixed indoor temperature of 27 °C.

Active cooling systems	Outdoor temperature (T_{out}) [°C]	Total cooling capacity (P_c) [kW]	Energy Efficiency Ratio (EER)
Split system – 1	35	3.5	3.35
	30	2.41	5.21
	25	1.57	8.81
	20	1.31	12.85
Split system – 2	35	9.5	3.59
	30	7.03	5.83
	25	4.46	8.18
	20	3.31	13.03
Multi-split system – 1	35	22	3.31
	30	16.2	4.69
	25	10.4	8.22
	20	5.28	13

factors share similarities, it is noteworthy that the Indoor Temperature Influence Factor (W) exhibits a shallower slope, precisely half as steep as the Indoor Temperature Influence Factor (Q).

$$EER = \frac{Q}{W} \tag{15}$$

$$W_{target}(T_{in}, T_{out}) = \frac{Q_{designc}.PartLoadFactor(T_{out})}{EER * IndoorTemperatureinfluencefactor\ (W)\ (T_{in})} \tag{16}$$

To assess the accuracy of the present paper model parameters and target values, Fig. 5 presents a detailed overview of the EER values for the split system – 1. This chart encompasses a wide range of outdoor temperatures while considering different indoor temperature settings during system operation. The model results demonstrate that at the manufacturer's declared indoor temperature of 27 °C, the EER values at the four different outdoor temperatures (35, 30, 25, and 20) °C are identical in both the model and the manufacturer's data as marked in the figure.

2.6. Cooling systems sensitive sizing and design

In this study, the adaptation of split system sizing was based on a climate change-sensitive approach. The sizing was conducted separately for various weather files representing different periods and SSP scenarios. The process involved defining "design days" to determine the cooling that will be exceeded on 5%, 2%, and 1% of days.

This method is guided by the ISO 15927-2 standard [76]. The study used hourly temperature data (dry bulb temperature) and hourly total global solar irradiation values. The daily mean values for both parameters were calculated, and percentiles for three percentages (99%, 98%, and 95%) were determined for each month and parameter (temperature and global solar irradiance). Initial intervals were established by adding and subtracting 0.5 for temperature and 0.05 for irradiance to the calculated percentiles. The goal is to identify a single day per month that falls within both intervals, making it the design day. If multiple days met the criteria, a selection process was used to determine the unique design day. The highest temperature of the hottest design day for the 99% percentile was chosen as the maximum outdoor temperature for sizing.

Table 3 provides the maximum dry bulb temperatures for the design day under various scenarios for the design day weather data. This sizing approach ensures that split system sizing accounts for the impacts of climate change and varying scenarios, making it more resilient to future environmental changes.

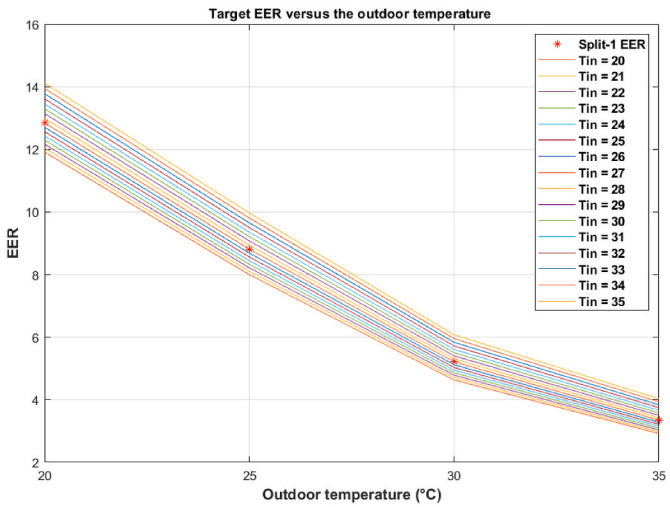

Fig. 5. EER values versus the outdoor temperatures in different indoor temperatures operating conditions for split system – 1.

Table 3
Design day weather data based on ISO 15927-2 standard [76] for different TMYs and different SSP scenarios.

Scenarios (TMYs)	Design day weather data (maximum dry bulb temperature) [°C]
2010s	36.9
2050s_SSP2-4.5	39.6
2050s_SSP3-7.0	39.6
2050s_SSP5-8.5	38.2
2090s_SSP2-4.5	38.9
2090s_SSP3-7.0	42.9
2090s_SSP5-8.5	41.9

3. Results

3.1. Evolution of outdoor climate conditions

The results show that the projected outdoor temperature changes for three SSP scenarios over two future TMYs, the 2050s and the 2090s, were examined in relation to the reference TMY in the 2010s. Fig. 6 indicates significant temperature increases. Between the 2010s and 2050s, all three SSP scenarios show warming trends across the months, with SSP5-8.5 projecting the highest temperature increases. Notably, in the SSP5-8.5 scenario, January temperatures are projected to rise by 2.1 °C and July temperatures by an alarming 2.7 °C. The difference in temperatures between the 2010s and 2050s ranges from 0.3 °C to 2.7 °C across the scenarios and months. Extending the analysis to 2090, the warming trends become even more pronounced. January temperatures are projected to increase by 3.7 °C in SSP2-4.5, while July temperatures could increase by 3.8 °C and 4.1 °C in SSP3-7.0 and SSP5-8.5, respectively. Overall, the temperature differences between the 2010s and the 2090s vary from 1.3 °C to 4.1 °C.

Additionally, in this study, three distinct heatwaves were examined, each occurring within different timeframes: "HW [2001–2020]" in 2019, "HW [2040–2060]" in 2054, and "HW [2080–2100]" in 2083. These three studied heatwaves are characterized by specific durations, outdoor air temperature thresholds, and associated meteorological variables. Fig. 7 shows the average hourly outdoor temperature profiles during the three distinct heatwaves. Of particular significance is the heatwave in "Heatwave [2081–2100]," which stands out with its notable temperature patterns. In this heatwave, daytime temperatures exhibit a substantial increase, with the afternoon temperatures consistently exceeding those observed in the earlier heatwaves. The maximum average hourly temperature during this late 21st-century heatwave notably reaches its zenith at 39.6 °C. In comparison, the maximum hourly outdoor temperatures for "Heatwave [2001–2020]" and "Heatwave [2041–2060]" are 35.7 °C and 36.4 °C, respectively.

Fig. 8 represents the hourly outdoor air temperature data recorded during the three heatwaves with the highest maximal temperature detected in the respective years. The "HW [2001–2020]" heatwave, occurring in 2019, persisted for five days from 25 June to 29 June, as shown in Fig. 8 (a). During this period, outdoor air temperatures exceeded various threshold levels, with temperatures surpassing 30 °C for 39% of the time, 35 °C for 24% of the time, and 40 °C for 3% of the time. The maximum temperature reached 41.0 °C, while the minimum temperature during the heatwave was 15.2 °C, resulting in an average temperature of 28.6 °C.

The "HW [2040–2060]" heatwave, manifesting in 2054, endured for nine days from 02 August to 10 August, as shown in Fig. 8 (b). During this episode, outdoor air temperatures were notably elevated, with temperatures exceeding 30 °C for 41% of the time, 35 °C for 17% of the time, and 40 °C for 3% of the time. The maximum temperature reached 43.1 °C, and the minimum temperature was 14.6 °C, leading to an average temperature of 27.9 °C.

The "HW [2080–2100]" heatwave, occurring in 2083, spanned seven days from 26 June to 02 July, as shown in Fig. 8 (c). This heatwave exhibited elevated temperature levels, with temperatures surpassing

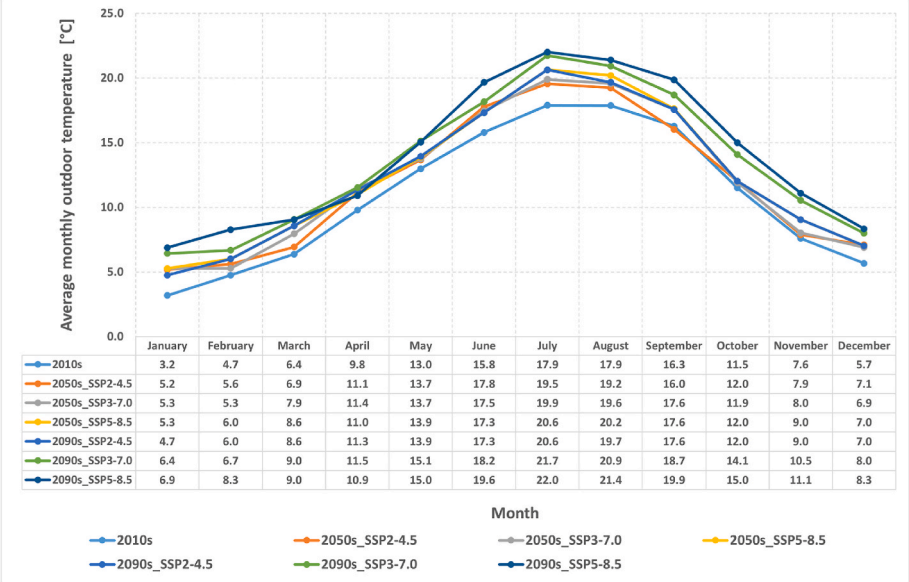

	January	February	March	April	May	June	July	August	September	October	November	December
2010s	3.2	4.7	6.4	9.8	13.0	15.8	17.9	17.9	16.3	11.5	7.6	5.7
2050s_SSP2-4.5	5.2	5.6	6.9	11.1	13.7	17.8	19.5	19.2	16.0	12.0	7.9	7.1
2050s_SSP3-7.0	5.3	5.3	7.9	11.4	13.7	17.5	19.9	19.6	17.6	11.9	8.0	6.9
2050s_SSP5-8.5	5.3	6.0	8.6	11.0	13.9	17.3	20.6	20.2	17.6	12.0	9.0	7.0
2090s_SSP2-4.5	4.7	6.0	8.6	11.3	13.9	17.3	20.6	19.7	17.6	12.0	9.0	7.0
2090s_SSP3-7.0	6.4	6.7	9.0	11.5	15.1	18.2	21.7	20.9	18.7	14.1	10.5	8.0
2090s_SSP5-8.5	6.9	8.3	9.0	10.9	15.0	19.6	22.0	21.4	19.9	15.0	11.1	8.3

Fig. 6. Average monthly outdoor temperature in Brussels based on MAR forced by BCC-CSM2-MR ESM.

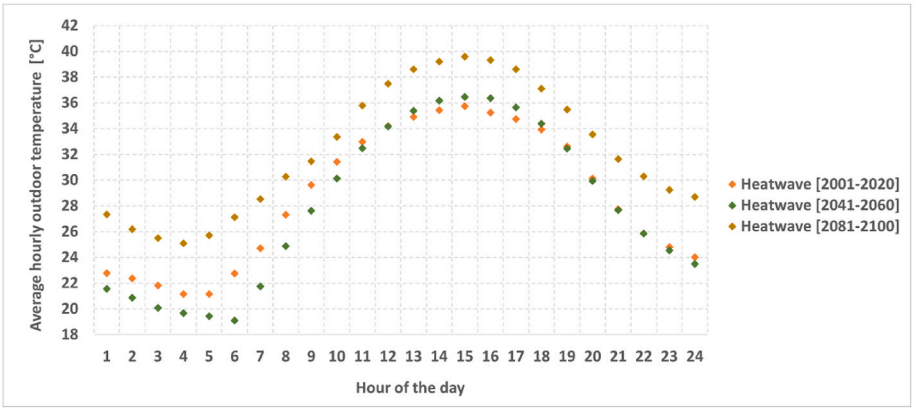

Fig. 7. Average hourly outdoor temperature during heatwaves.

30 °C for 57% of the time, 35 °C for 35% of the time, and 40 °C for 19% of the time. The maximum temperature during this heatwave reached an unprecedented 46.0 °C, while the minimum temperature was 18.7 °C, resulting in an exceptionally high average temperature of 32.3 °C. Table 4, on the other hand, provides a comprehensive summary of the primary parameters associated with these three heatwaves.

3.2. Evolution of thermal comfort indicators

In this study, the results show that IOhD varies across different building types and in different weather scenarios, with a focus on the impact of varying ventilation and cooling systems, as shown in Fig. 9. Three scenarios are explored: Scenario 1, featuring mechanical ventilation (MV); Scenario 2, where natural ventilation (NV) is introduced alongside MV; and Scenario 3, incorporating a split system for active cooling.

In scenario 1 (MV), the IOhD for freestanding buildings saw substantial increases, with an increase of up to 176% in the 2050s and 477% in the 2090s compared to the 2010s. Semi-detached buildings exhibited a similar trend, with increases of 203% in the 2050s and 586% in the 2090s. Terraced buildings experienced notable growth in IOhD, particularly in the 2050s, peaking at 257%. Apartments, on the other hand, demonstrated milder increases in IOhD, with 89% in the 2050s and 259% in the 2090s.

In Scenario 2 (MV and NV), the IOhD increased further. Freestanding and semi-detached buildings maintained their positions with the highest increases by the 2090s. Freestanding structures reached a maximum IOhD increase of 164% in the 2050s and 403% in the 2090s, and semi-detached buildings observed a peak of 177% in the 2050s and 438% in the 2090s. Terraced houses showed the highest IOhD increase in the 2050s to 257%, while apartments experienced a rise of 144% in the 2050s and 337% in the 2090s.

However, the most intriguing results emerged in scenario 3 (MV, NV, and Split system). In this scenario, IOhD levels are remarkably close to zero in the different building types by the 2050s and the 2090s. The results presented here are based on the TMY weather scenarios.

The study not only considers the impact of different TMY scenarios on IOhD but also provides insights into indoor operational temperature (IOpT) during heatwaves, shedding light on how these scenarios affect thermal comfort. In addition to IOhD, the results reveal the IOpT for two different building types: an average insulated freestanding building and an average non-insulated free-standing building, as shown in Fig. 10. These findings are particularly significant in the context of the longest heatwave among the three studied, which will occur in 2054 and will last for nine days.

For the insulated building, the results demonstrate variations in IOpT

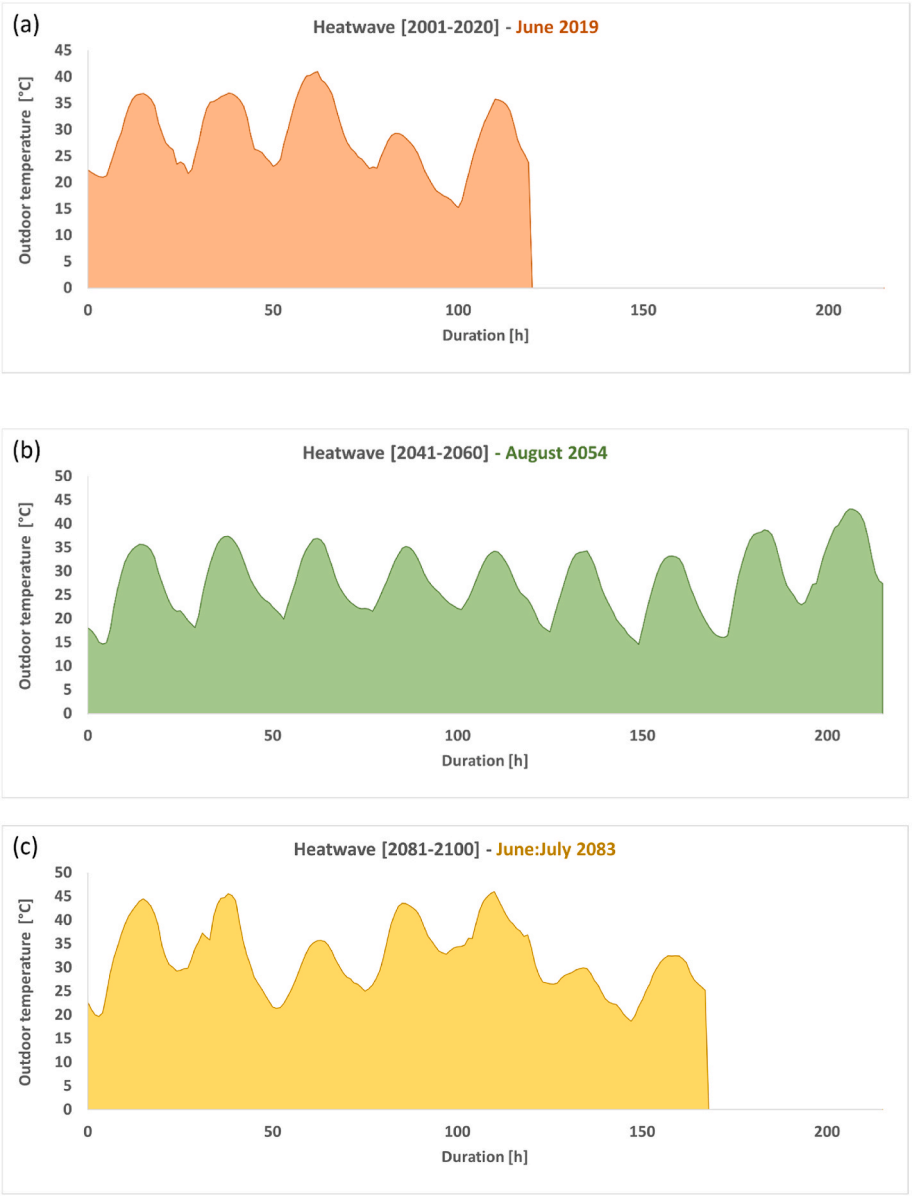

Fig. 8. Hourly outdoor air temperature during the highest maximal temperature heatwaves detected in 2019 for the [2001–2020] period, 2054 for the [2041–2060] period, and 2083 for the [2081–2100].

across different cooling scenarios. The maximum IOpT values reach 39.5 °C, 36.3 °C, and 30.2 °C in scenarios involving MV only, MV combined with NV, and MV, NV, and a split cooling system, respectively. Conversely, the non-insulated building experiences even higher IOpT values during the same heatwave, further emphasizing the importance of cooling strategies. In this case, the maximum IOpT peaks at 44.3 °C, 43.1 °C, and 32.0 °C for scenarios with MV only, MV and NV, and MV, NV, and a split system.

The results underscore a critical challenge in ensuring indoor thermal comfort during heatwaves, even with advanced cooling systems like the split system. It becomes evident that the IoPT often exceeds the desired cooling set point temperature of 26 °C, indicating that the initial cooling system sizing, typically based on design days within the TMY, falls short during extreme heat events. To address this issue, this study also explores an innovative approach – resizing the split system based on the highest temperature recorded during the heatwave.

In Fig. 11, the results exemplify the benefits of this resizing strategy. For an insulated freestanding building, the maximum IOpT before resizing reaches 30.2 °C, significantly surpassing the set point temperature. However, through the adaptation of the split system based on the peak heatwave temperature, which in this case is 43.1 °C, a remarkable transformation occurs. The maximum IOpT post-resizing is reduced to 26.4 °C, with only 0.4 °C above the intended cooling set point temperature.

Furthermore, the study reveals an intriguing aspect of the resizing process during heatwave periods, particularly in the context of future climate scenarios. Notably, the findings suggest that in the 2090s and, to some extent, in the 2050s, the optimal solution occasionally involves transitioning to a larger-capacity cooling system. This evolution necessitates a shift from a smaller-capacity (3.5 kW) split system to a medium-capacity (9.5 kW) split system or even from a medium-capacity split system to a larger-capacity (22 kW) split system, as shown in Table 5.

3.3. Evolution of final cooling energy consumption and GHG emissions

The results of this study show a significant shift in cooling energy demand due to the projected weather scenarios for the 2050s and 2090s in comparison to the 2010s. As shown in Fig. 12, the distribution of split

Table 4
Main parameters of the three studied heatwaves with the highest maximal temperature.

		HW [2001–2020] (2019)	HW [2040–2060] (2054)	HW [2080–2100] (2083)
Duration [days]		5	9	7
Date		25 June-29 June	02 August-10 August	26 June-02 July
Percentage of time when the outdoor air temperature is above [%]	26 [°C]	62%	57%	80%
	30 [°C]	39%	41%	57%
	35 [°C]	24%	17%	35%
	40 [°C]	3%	3%	19%
Maximum temperature [°C]		41.0	43.1	46.0
Minimum temperature [°C]		15.2	14.6	18.7
Average temperature [°C]		28.6	27.9	32.3

systems across these future scenarios indicates the transformation in the capacity requirements. In the 2010s, small-capacity systems (3.5 kW) played a dominant role, representing 40% of the installed systems, while medium-capacity systems (9.5 kW) also accounted for 40%, and large-capacity systems (22 kW) constituted 20%.

However, the subsequent decades reveal a distinct pattern. In the 2050s, there is a clear decline in the share of small-capacity systems, reducing to 37%, signifying a shift in response to the rising cooling demand. While medium-capacity systems remain consistent, maintaining their 40% share, suggesting their adaptability to the changing climate conditions. Meanwhile, large-capacity systems demonstrate substantial growth, increasing to 23%. This expansion continues into the 2090s, where the share of small-capacity systems further diminishes to 22%, medium-capacity systems rise to 46%, and large-capacity systems increase to 32%.

Additionally, the results show the distribution of the split systems among the different building types in the 2090s. In apartment buildings, the small capacity split system (3.5 kW) stands out with the highest share, constituting 44% in the 2090s. Conversely, semi-detached and terraced buildings consistently favour medium-capacity split systems (9.5 kW), with semi-detached structures maintaining the highest share across the years. In contrast, freestanding houses are inclined toward large-capacity split systems (22 kW).

The results presented in Fig. 13 provide a comprehensive overview of the changes in cooling and ventilation final energy consumption within the entire building stock for different climate scenarios over the course of the century. In the 2050s, under SSP2-4.5, SSP3-7.0, and SSP5-8.5, the cooling consumption exhibited a substantial increase, with percentages ranging from 106% to 141% compared to the 2010s. Similarly, the ventilation energy consumption also witnessed significant growth, with an increase between 37% and 61% for the same period.

As we transition to the 2090s, the magnitude of change becomes even more pronounced. The cooling energy consumption shows a remarkable escalation, with SSP2-4.5 recording a 174% increase, SSP3-7.0 experiencing a 221% surge, and SSP5-8.5 reaching an astonishing 280% rise. The ventilation energy consumption parallels these trends, with percentages soaring to 131%, 165%, and 197%, respectively.

The third cooling scenario, which employs split cooling systems, is particularly noteworthy for its high electricity consumption, contributing significantly to the overall GHG emissions. This is further compounded by the mechanical ventilation systems, which also rely on electricity for operation. The results presented in Fig. 14 offer a profound insight into the evolving landscape of GHG emissions, showcasing the dramatic changes in emission levels within the building sector. In the 2010s, GHG emissions were recorded at 106,438 tons for the current state, which included 3874 tons attributed to mechanical ventilation systems.

The 2050s reveal a significant increase in GHG emissions under various SSPs. In SSP2-4.5, emissions surged to 216,581 tons, with 5314 tons associated with mechanical ventilation systems. In SSP3-7.0, emissions reached 245,125 tons, including 6014 tons from mechanical ventilation, while in SSP5-8.5, emissions peaked at 253,608 tons, with 6222 tons originating from mechanical ventilation and active cooling systems.

In the 2090s, under SSP2-4.5, GHG emissions dramatically increased to 289,881 tons, with 8960 tons stemming from mechanical ventilation systems. SSP3-7.0 witnessed a surge to 339,571 tons, of which 10,270 tons were attributed to mechanical ventilation, while SSP5-8.5 demonstrated the highest emissions, peaking at 401,655 tons.

4. Discussion

4.1. Findings and recommendations

The significant increase in global temperatures is a well-documented phenomenon driven primarily by the accumulation of greenhouse gases in the atmosphere. This trend, set to continue in the coming decades, necessitates adaptive strategies to counteract the adverse effects of heatwaves, as reported in previous studies [77,78], which can be severe, particularly in urban areas. As urbanization intensifies, the urban heat island affects further local temperature conditions, making the need for cooling systems even more imperative. The IPCC's comprehensive reports indicate that if emissions continue to escalate at their present rates, global temperatures could surge within a wide range, spanning from 1 to 5.7 °C by the close of this century. The variance in this temperature range is primarily contingent upon the SSP scenarios followed. To address this trajectory, this paper explores the implications of varying SSP scenarios.

This study utilized the MAR model, renowned for its ability to enhance the spatial and temporal resolution of weather data. Operating at a remarkable 5 km spatial resolution, MAR significantly refines our understanding of climate patterns, allowing us to assess the impacts of climate change at a finer scale. Historical simulations (1980–2014) were based on the ERA5 reanalysis dataset, closely approximating observed climate conditions. The simulations then progressed to the 2015–2100 period, driven by three ESMs, including the BCC-CSM2-MR model. These ESMs illustrate the mean evolution of climate under varying carbon emissions scenarios, specifically, the SSPs. The SSP5-8.5 scenario was chosen as a basis to reconstruct the SSP3-7.0 and SSP2-4.5 scenarios, three of which are used in this study. Within the study, the incorporation of TMY datasets allowed for a thorough examination of synthetic hourly data.

Between the 2010s and 2050s, all three SSP scenarios exhibited significant warming trends across the months. However, it is particularly striking that the SSP5-8.5 scenario projects the highest temperature increases. This scenario foresees a substantial rise in temperatures, with January temperatures expected to increase by 2.1 °C and July temperatures by a considerable 2.7 °C. These temperature differences range from 0.3 °C to 2.7 °C when comparing the 2010s to the 2050s across the various scenarios and months. As the analysis extends to the 2090s, the warming trends become even more pronounced. January temperatures could increase by 3.7 °C in the SSP2-4.5 scenario, while July temperatures are forecasted to rise significantly by 3.8 °C in SSP3-7.0 and 4.1 °C in SSP5-8.5. These projections are indicative of an alarming warming trend that extends throughout the year, presenting serious challenges in terms of climate resilience and adaptation efforts, as reported in a previous study by Amaripadath et al. [7]. Overall, the temperature differences between the 2010s and the 2090s vary from 1.3 °C to 4.1 °C, underlining the urgency of addressing climate change and its potential impacts on the built environment and cooling strategies.

The study also focused on understanding heatwaves and acknowledging their influence on cooling strategies. The definition of heatwaves

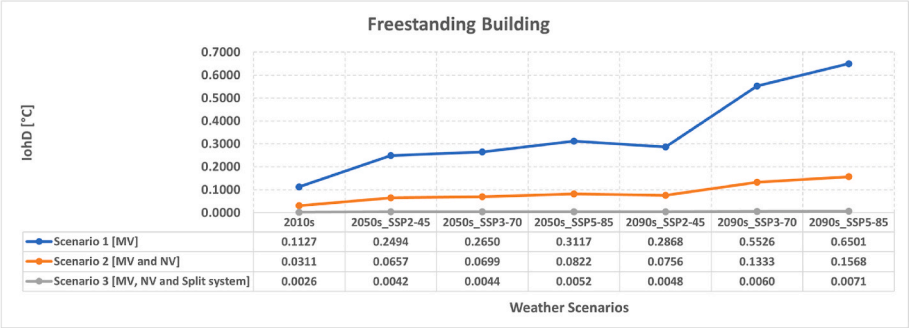

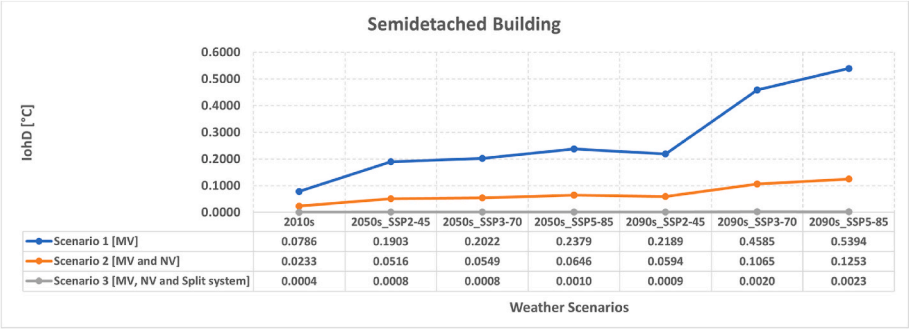

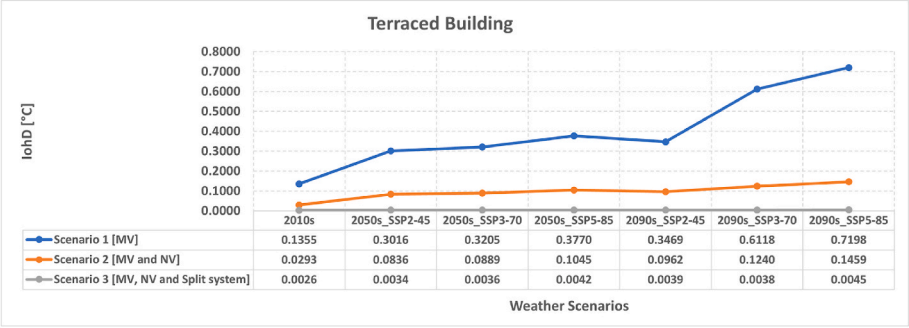

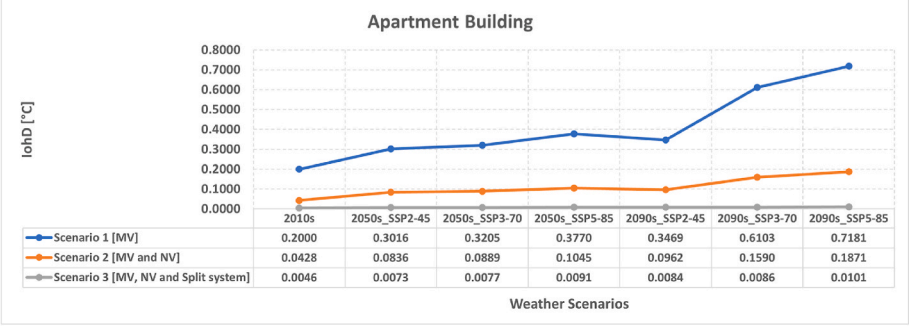

Fig. 9. Average IohD presented by weather scenarios for the different building types.

in Belgium, influenced by the Royal Meteorological Institute, involves specific temperature criteria and duration thresholds. To capture the local climate nuances, the study adopted an alternative heatwave definition, accounting for characteristics unique to each region. This approach is rooted in another framework that classifies heatwave events based on duration, maximal temperature, and overall intensity. It is a crucial step toward assessing heatwave events in a more region-specific and relevant manner. The study focused on heatwaves occurring during three distinct time frames: 2001–2020 (representing historical scenarios), 2041–2060 (mid-future scenarios), and 2081–2100 (projected future scenarios).

A notable highlight is the “Heatwave [2081–2100]," which demonstrates distinct temperature patterns. This late 21st-century heatwave is characterized by substantially increased daytime temperatures, with afternoon temperatures consistently surpassing those observed in the earlier heatwaves. The “HW [2001–2020]" in 2019 endured for five days, with temperatures frequently exceeding 30 °C, 35 °C, and even 40 °C. The maximum temperature during this heatwave reached 41.0 °C. The “HW [2040–2060]" in 2054 was more extended, spanning nine days and reaching a maximum temperature of 43.1 °C. The “HW [2080–2100]" in 2083 was the most extreme, with temperatures surpassing 40 °C for 19% of the time and peaking at a remarkable 46.0 °C. These findings underscore the escalating intensity and duration of heatwaves in the future, underscoring the critical importance of effective cooling strategies and building design to address these challenges.

In light of these challenges, the cooling demand in buildings is poised

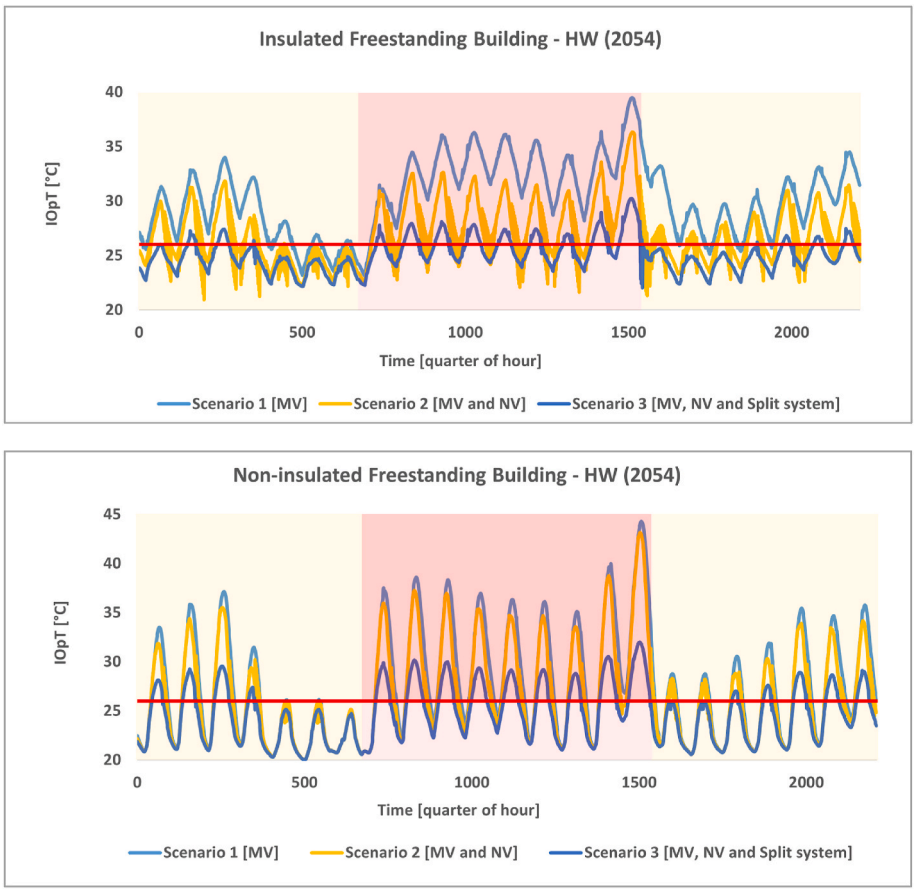

Fig. 10. Indoor operative temperature (IOpT) for an insulated and non-insulated freestanding building during the heatwave (HW) of 2054 in the three scenarios (including one week shoulder period).

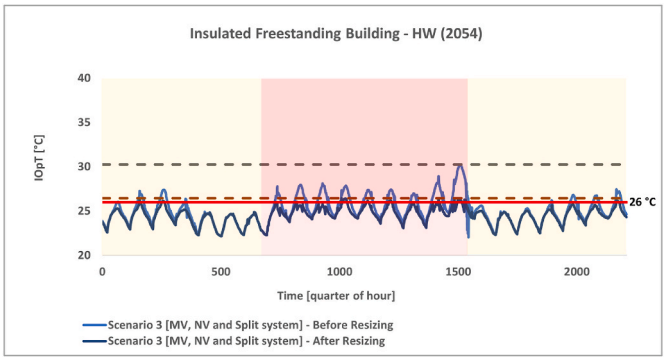

Fig. 11. Indoor operative temperature (IOpT) for an insulated freestanding building during the heatwave (HW) of 2054 in scenario 3 before and after resizing the split system (including one week shoulder period).

to rise significantly, as reported by the IEA [6,14], compelling us to reconsider the traditional approaches to space cooling. The projections for the future are unequivocal, with even higher cooling requirements expected due to elevated temperatures. These changes make it imperative for building designers, engineers, and policymakers to prioritize the integration of effective cooling strategies to maintain occupant comfort and health. This study introduces and evaluates three distinct cooling strategies within the building stock. These strategies include (mechanical ventilation), (mechanical ventilation and natural ventilation), and (mechanical ventilation, natural ventilation, and split systems). The first strategy focuses on the incorporation of mechanical ventilation systems to enhance thermal comfort. The second approach combines mechanical ventilation with natural ventilation, optimizing the balance between energy efficiency and occupant comfort. The third and most advanced strategy integrates mechanical ventilation and natural ventilation systems with active cooling in the form of split systems, offering a multi-faceted approach to cooling that ensures adaptability to varying environmental conditions and occupant needs. These strategies underscore the importance of a holistic approach to cooling solutions in maintaining indoor comfort, improving energy efficiency, and addressing the evolving needs of building environments due to climate change.

The study investigates IOhD as a measure of thermal comfort across different building types and weather scenarios, focusing on the impact of varying ventilation and cooling systems. Three scenarios are explored: Scenario 1 (MV), Scenario 2 (MV and NV), and Scenario 3 (MV, NV, and Split system). In Scenario 1 (MV), significant IOhD increases are observed, with freestanding and semi-detached buildings experiencing the highest growth, reaching up to 586% in the 2090s for semi-detached buildings. Terraced and apartment buildings also show substantial IOhD increases. In Scenario 2, incorporating natural ventilation (NV) alongside mechanical ventilation (MV), IOhD values consistently decrease across various building types, with a maximum value of 0.2 by the 2090s. This highlights the efficacy of combining MV and NV to enhance thermal comfort and reduce IOhD values. Natural ventilation proves to be a sustainable, energy-efficient cooling solution that mitigates heat-related discomfort, promoting occupant well-being and emphasizing the importance of its integration in future building designs. Remarkably, Scenario 3 (MV, NV, and split system) shows IOhD levels approaching zero across different building types by the 2050s and 2090s, highlighting the effectiveness of active cooling systems. These results, based on the TMY weather scenarios, signify the potential of active cooling systems to enhance thermal comfort in the face of climate change

Table 5
Split systems resizing for the different building types during the three studied heatwaves.

Building type	Insulation	Split system capacity [kW]					
		2010s		2050s		2090s	
		Before resizing	After resizing	Before resizing	After resizing	Before resizing	After resizing
Freestanding	Insulated	3.5	3.5	3.5	9.5	3.5	9.5
	Non-insulated	22	22	22	22	22	22
Semi-detached	Insulated	3.5	3.5	3.5	3.5	3.5	9.5
	Non-insulated	22	22	22	22	22	22
Terraced	Insulated	3.5	3.5	3.5	3.5	3.5	9.5
	Non-insulated	22	22	22	22	22	22
Apartment	Insulated	3.5	3.5	3.5	3.5	3.5	3.5
	Non-insulated	9.5	9.5	9.5	9.5	9.5	9.5

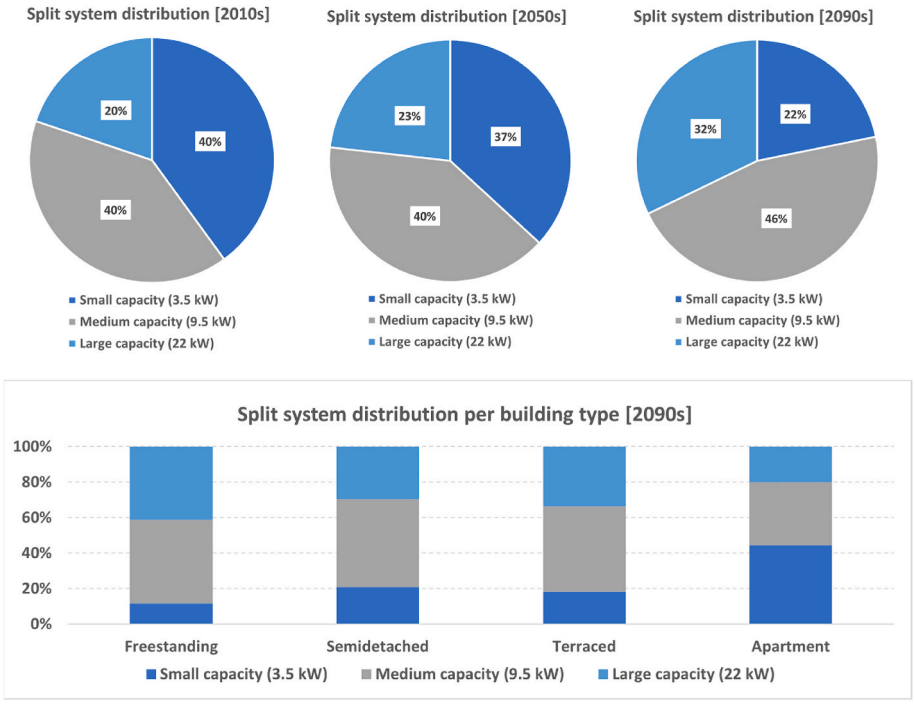

Fig. 12. Distribution of split systems in the different TMYs and per building type in the 2090s in SSP5-8.5.

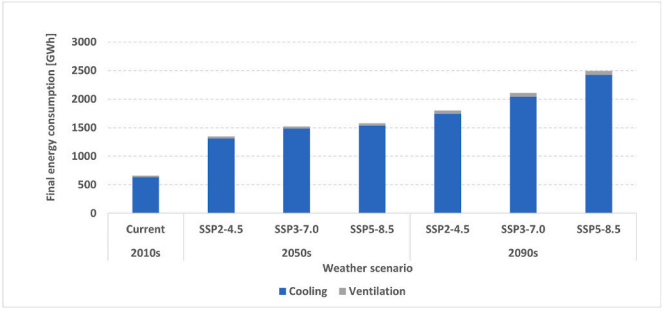

Fig. 13. Final energy consumption for cooling and ventilation systems in the different weather scenarios for the entire building stock.

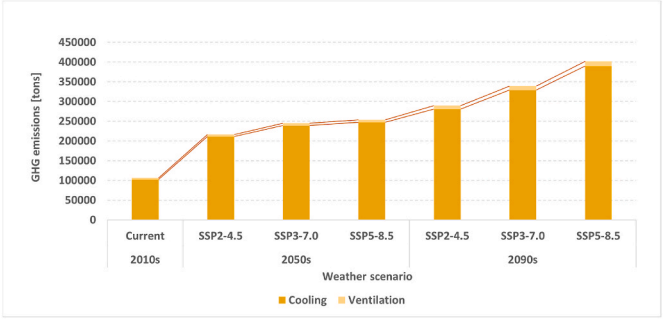

Fig. 14. GHG emissions for cooling and ventilation systems in the different weather scenarios for the entire building stock.

challenges.

The study's evaluation of IOpT during heatwaves offers valuable insights into the impact of cooling scenarios on thermal comfort during heatwaves. In the 2054 heatwave, variations in IOpT are evident, especially between insulated and non-insulated buildings. For insulated buildings, maximum IOpT values remain below 40 °C in all scenarios. In contrast, non-insulated buildings experience higher IOpT up to 44.3 °C.

The study highlights the growing importance of effective cooling measures to ensure occupant comfort during the intensifying heatwaves. However, a critical observation is that even with the three implemented cooling strategies, thermal comfort standards during heatwaves remain unmet. This indicates a crucial issue related to the sizing of cooling systems, including active cooling systems like the split system. The failure to achieve thermal comfort standards during heatwaves, despite the combination of mechanical ventilation, natural ventilation, and active cooling, raises concerns about the appropriateness of the sizing

methods for cooling systems, especially when dealing with extreme heat events. It underscores the necessity for a more robust approach that considers the highest temperature conditions during heatwaves, ensuring that cooling systems are adequately sized to meet occupants' needs and well-being under these challenging circumstances. In an insulated freestanding building, the initial cooling split system struggled to maintain indoor temperatures within the set point during a heatwave, reaching a high of 30.2 °C. However, resizing the system based on the peak heatwave temperature, which hit 43.1 °C, resulted in a remarkable improvement. The resizing maximum temperature dropped significantly to 26.4 °C, just 0.4 °C above the target set point. This approach has the potential to substantially enhance thermal comfort during extreme heatwaves.

The study's results reveal a substantial shift in cooling energy demand in response to future weather scenarios in the 2050s and 2090s compared to the 2010s. There is an increase in cooling and ventilation energy consumption. In the 2050s, cooling consumption increases by 106%–141%, and ventilation energy consumption grows by 37%–61% across different climate scenarios. The 2090s see even more significant changes, with cooling energy consumption surging by 174%–280% and ventilation energy consumption increasing by 131%–197%.

The study also emphasizes the substantial impact of split cooling systems and mechanical ventilation on GHG emissions in the building sector. In the 2010s, GHG emissions totalled 106,438 tons, with 3874 tons attributed to mechanical ventilation. Transitioning to the 2050s, emissions surged across SSPs, reaching 253,608 tons (6222 tons from mechanical ventilation) in SSP5-8.5. Moving to the 2090s, SSP5-8.5 exhibited the highest emissions at 401,655 tons. These findings highlight the urgency of addressing the surging GHG emissions within the building sector.

The list below is given as a summary of the main findings and recommendations.

1. Global temperatures are projected to increase significantly due to greenhouse gas accumulation, particularly in urban areas where heatwaves can have severe effects. The severity of temperature rise depends on emissions scenarios, with a range of 1–5.7 °C by the end of the century.
2. The study explores different emissions scenarios using advanced climate models and focuses on the impact of climate change on heatwaves. It identifies an alarming trend of intensifying heatwaves, which will challenge climate resilience and adaptation efforts.
3. With the growing need for cooling in buildings, the study introduces three cooling strategies: mechanical ventilation, a combination of mechanical and natural ventilation, and a more advanced system that includes active cooling. The advanced system shows promise in enhancing thermal comfort.
4. The study reveals that even with these cooling strategies, thermal comfort standards are not met during heatwaves. This highlights concerns about the sizing of cooling systems and the need for more robust approaches to ensure occupant well-being during extreme heat events.
5. As global temperatures rise, the study anticipates a substantial increase in cooling and ventilation energy consumption, underscoring the urgency of addressing this issue with passive cooling strategies.

4.2. Strengths and limitations

This study possesses several notable strengths. Firstly, it relies on weather data derived from the MAR model, renowned for its high spatial resolution and detailed parameterization tailored to the specific region of Belgium, ensuring the validity of climate data for simulations. Secondly, the study's innovative climate-sensitive approach in selecting and sizing HVAC systems based on the ISO 15927-2 standard ensures that the chosen systems are suitable for various weather scenarios, ultimately improving thermal comfort. Thirdly, the application of a multi-zonal building stock model, previously validated in our previous research by Elnagar et al. [25], offers a highly detailed and accurate representation of each building within the building stock, facilitating precise calculations of indoor conditions and cooling energy demands. Lastly, the use of the IOhD indicator for assessing thermal comfort in various weather scenarios under different cooling strategies adds depth and comprehensiveness to the study's insights. These strengths collectively bolster the study's credibility and its potential to inform strategies related to cooling technologies, thermal comfort, and the impact on energy consumption and greenhouse gas emissions in building stocks.

However, the study has some limitations. Firstly, it focuses on a limited number of periods (2010s, 2050s, and 2090s) and a specific set of SSPs, omitting intermediate timeframes (e.g., 2030s, 2040s, 2060s, etc.) and alternative SSP scenarios that could provide a more comprehensive understanding of climate impacts (e.g., SSP1-1.9 "very low GHG emissions" and SSP1-2.6 "low GHG emissions"). The study's second limitation pertains to the omission of cooling systems in the classification of residential building stock. In temperate climate regions such as Belgium, the adoption of active air conditioning systems in residential buildings has been relatively uncommon or unnecessary in recent years. Additionally, the use of weather data representative of Brussels for the entire building stock assumes it represents the entirety of Belgium, potentially overlooking local weather variations between different regions. Lastly, the study employs ISO 13790:2007 for building modelling, a method that has been succeeded by the more detailed ISO 52016–1, which the study didn't incorporate due to its initiation prior to the introduction of the new standard. These limitations suggest opportunities for further research.

4.3. Implications on practice and future research

The findings of this study offer significant implications for both practical applications and avenues for future research.

- **Practical Implications:**
  1. **Cooling Strategies:** With the imminent rise in global temperatures, the study underscores the urgency of adopting cooling strategies, especially in urban areas. This involves a shift from traditional cooling methods to more advanced approaches that incorporate mechanical ventilation, natural ventilation, and active cooling systems. Building designers, engineers, and policymakers should prioritize these strategies to maintain indoor comfort and occupant health as temperatures continue to surge.
  2. **Heatwave Resilience:** The intensifying heatwaves, as revealed in the study, call for innovative heatwave-resilient building designs. These designs should focus on enhancing thermal comfort during extreme heat events. A crucial recommendation is the need for more robust approaches to sizing cooling systems, ensuring they can effectively meet occupants' needs and well-being during such challenging conditions.
  3. **Reducing Greenhouse Gas Emissions:** The study highlights the substantial impact of split cooling systems and mechanical ventilation on greenhouse gas emissions in the building sector. To mitigate this, practitioners should explore passive cooling strategies and energy-efficient building designs that reduce emissions while ensuring occupant comfort.
- **Future Research Directions:**
  1. **Intermediate Periods and Additional SSP Scenarios:** Future research should address the limitation of this study by exploring intermediate timeframes (e.g., 2030s, 2040s, 2060s) and considering a wider range of Shared Socioeconomic Pathways (SSPs), including scenarios with very low and low greenhouse gas emissions. This would provide a more comprehensive understanding of climate impacts and adaptive strategies.
  2. **Localized Weather Data:** Given the assumption that Brussels weather data represents all of Belgium, future studies could

benefit from utilizing more localized weather data to account for regional variations. Analyzing different cities or regions within a country would offer insights into localized climate nuances.

3. **Updated Building Modelling Standards:** As building modelling standards evolve, future research should adapt to the most current standards. Transitioning from ISO 13790:2007 to ISO 52016–1 or other updated standards would enhance the accuracy of building energy simulations and improve the precision of findings.
4. **Sustainable** and **Passive Cooling Technologies:** Investigating the efficacy of sustainable and passive cooling strategies alongside active systems can provide a holistic approach to reducing energy consumption and greenhouse gas emissions. Future studies could focus on designs that integrate renewable energy sources, energy-efficient materials, and architectural innovations.

5. Conclusion

The global climate is undergoing a significant transformation, marked by the unequivocal rise in temperatures primarily driven by the accumulation of greenhouse gases in the atmosphere. This alarming trend is expected to persist in the coming decades, necessitating proactive and adaptive cooling strategies to mitigate the adverse consequences of this change. This research addresses the pressing need to integrate various cooling strategies into the building stock, particularly in the face of rising global temperatures. The study has explored the impact of these strategies on thermal comfort, final energy consumption, and GHG emissions. The results indicate that while advanced cooling strategies hold promise in enhancing thermal comfort, significant challenges remain in meeting thermal comfort standards during extreme heatwaves. The study also underscores the need for a more robust approach to sizing cooling systems, especially when dealing with these extreme heatwaves. It is concluded that.

- The study reveals alarming temperature increases from the 2010s–2050s and 2090s, particularly under the SSP5-8.5 scenario, with potential rises of up to 4.1 °C.
- The “Heatwave [2081–2100]" stands out with its alarming temperature patterns. It is characterized by significantly higher daytime temperatures, peaking at a remarkable 46.0 °C, compared to earlier heatwaves. In contrast, the “HW [2001–2020]" peaked at 41.0 °C, and the “HW [2040–2060]" at 43.1 °C.
- In Scenario 1 (MV), IOhD increased significantly, up to 586% in the 2090s, compared to the 2010s for semi-detached buildings. Scenario 2 (MV and NV) consistently reduced IOhD, reaching a maximum value of 0.2 °C by the 2090s. Scenario 3 (MV, NV, and Split system) achieved near-zero IOhD in various building types by the 2050s and 2090s.
- In the 2054 heatwave, insulated buildings kept IOpT below 40 °C, while non-insulated ones reached 44.3 °C. Despite implementing three cooling strategies, thermal comfort standards were unmet, especially in non-insulated buildings.
- Inadequate cooling system sizing, even with active cooling, raises concerns, especially for extreme heat events. A more robust approach, considering peak heatwave temperatures, is essential to ensure occupant well-being. Resizing cooling systems based on the 43.1 °C peak temperature significantly improved performance, reducing the maximum indoor temperature to 26.4 °C, just 0.4 °C above the target.
- In the 2050s, cooling energy consumption increased by 106%–141%, and ventilation energy consumption rose by 37%–61% across various climate scenarios compared to the 2010s. In the 2090s, the changes were even more pronounced, with cooling energy consumption surging by 174%–280% and ventilation energy consumption growing by 131%–197%.
- In the 2010s, total GHG emissions were 106,438 tons, including 3874 tons from mechanical ventilation. By the 2050s, emissions reached 253,608 tons (with 6222 tons from mechanical ventilation) in SSP5-8.5. In the 2090s, SSP5-8.5 had the highest emissions at 401,655 tons.

CRediT authorship contribution statement

Essam Elnagar: Writing – review & editing, Writing – original draft, Visualization, Validation, Methodology, Investigation, Formal analysis, Data curation, Conceptualization. **Alessia Arteconi:** Writing – review & editing, Validation, Methodology, Conceptualization. **Per Heiselberg:** Writing – review & editing, Validation, Methodology, Conceptualization. **Vincent Lemort:** Writing – review & editing, Writing – original draft, Validation, Supervision, Project administration, Methodology, Investigation, Conceptualization.

Declaration of competing interest

The authors declare that they have no known competing financial interests or personal relationships that could have appeared to influence the work reported in this paper.

Data availability

Data will be made available on request.

Acknowledgement

This research was partially funded by the Walloon Region under the call ‘Actions de Recherche Concert’ees 2019 (ARC)’ (funding number: ARC 19/23–05) and the project OCCuPANt, on the Impacts Of Climate Change on the indoor environmental and energy PerformAnce of buildiNgs in Belgium during summer. The authors would like to gratefully acknowledge the Walloon Region and Liege University for funding. Computational resources have been provided by the Consortium des Équipements de Calcul Intensif (CÉCI), funded by the Fonds de la Recherche Scientifique de Belgique (F.R.S.-FNRS) under Grant No. 2.5020.11 and by the Walloon Region. This study is a part of the International Energy Agency (IEA) EBC Annex 80 – “Resilient cooling of buildings” project activities to define resilient cooling in residential buildings.

Appendix A

Table A. 1 summarizes the average coefficients of heat transmission (U-values) for the different building types and the different years of construction according to the insulation level. The source for the insulation values is according to, Tabula (value before renovation), LEHR (added insulation thickness for renovated elements of houses constructed before 1990), and EPB 2010 (for renovated elements of houses constructed after 1990) [44,53,79].

Table A. 1
Average U-values for the different types of buildings and different years of construction

Insulation		U_{wall} [W/m^{2}K]		$U_{windows}$ [W/m^{2}K]		U_{roof} [W/m^{2}K]		U_{floor} [W/m^{2}K]		U_{door} [W/m^{2}K]
		NI[1]	WI[2]	NI	WI	NI	WI	NI	WI	Mean
Year of construction	<1945	2.25	0.59	5	2.75	4.15	0.44	3.38	0.77	3.3
	1946–1970	1.56	0.53	5	2.75	3.33	0.43	3.38	0.77	3.3
	1971–1990	0.98	0.44	3.5	2.75	0.77	0.3	1.14	0.43	3.3
	1991–2007	0.49	0.4	3.5	2	0.43	0.3	0.73	0.4	3.3
	>2008	0.4		2		0.3		0.4		3.3

1 Not Insulated.
2 With Insulation.

Table A. 2 summarizes the average elements of total thermal capacity (K-values) for the different building types and the different years of construction according to the insulation level. The source for the insulation values is according to, Tabula (wall composition) and LEHR (added insulation thickness for renovated elements of houses constructed before 1990) [44,79].

Table A. 2
Average K-values for the different types of buildings and different years of construction

Insulation		K_{wall} [kJ/m^{2}K]		K_{roof} [kJ/m^{2}K]		K_{floor} [kJ/m^{2}K]	
		NI	WI	NI	WI	NI	WI
Year of construction	<1945	453.6	472.1	30.9	43.8	235.2	236.4
	1946–1970	483.9	502.4	42.6	55.5	235.2	236.4
	1971–1990	349.2	412.7	44.7	57.5	347.5	348.7
	1991–2007	396.2	414.8	46.7	50.9	348.1	349.2
	>2008	397.3		50.3		0.3	

References

[1] Climate Change, The Physical Science Basis. Contribution of Working Group I to the Sixth Assessment Report of the Intergovernmental Panel on Climate Change, Cambridge University Press, 2021, 2021.
[2] V. Eyring, S. Bony, G.A. Meehl, C.A. Senior, B. Stevens, R.J. Stouffer, et al., Overview of the coupled model Intercomparison project phase 6 (CMIP6) experimental design and organization, Geosci. Model Dev. (GMD) 9 (2016) 1937–1958, https://doi.org/10.5194/gmd-9-1937-2016.
[3] National Climate Commission, BELGIUM'S SIXTH NATIONAL COMMUNICATION on CLIMATE CHANGE - under the United Nations Framework Convention on Climate Change, 2013.
[4] United Nations - Climate Change, The Paris Agreement, 2015.
[5] N. Luo, Z. Wang, D. Blum, C. Weyandt, N. Bourassa, M.A. Piette, et al., A three-year dataset supporting research on building energy management and occupancy analytics, Sci. Data 9 (2022) 156, https://doi.org/10.1038/s41597-022-01257-x.
[6] International Energy Agency (IEA). Buildings - Energy System. IEA n.d. https://www.iea.org/energy-system/buildings (accessed August 27, 2023).
[7] D. Amaripadath, R. Rahif, W. Zuo, M. Velickovic, C. Voglaire, S. Attia, Climate change sensitive sizing and design for nearly zero-energy office building systems in Brussels, Energy Build. 286 (2023) 112971, https://doi.org/10.1016/j.enbuild.2023.112971.
[8] E. Elnagar, S. Pezzutto, B. Duplessis, T. Fontenaille, V. Lemort, A comprehensive scouting of space cooling technologies in Europe: key characteristics and development trends, Renew. Sustain. Energy Rev. 186 (2023) 113636, https://doi.org/10.1016/j.rser.2023.113636.
[9] E. Scoccimarro, O. Cattaneo, S. Gualdi, F. Mattion, A. Bizeul, A.M. Risquez, et al., Country-level energy demand for cooling has increased over the past two decades, Commun Earth Environ 4 (2023) 208, https://doi.org/10.1038/s43247-023-00878-3.
[10] R. Mutschler, M. Rüdisüli, P. Heer, S. Eggimann, Benchmarking cooling and heating energy demands considering climate change, population growth and cooling device uptake, Appl. Energy 288 (2021) 116636, https://doi.org/10.1016/j.apenergy.2021.116636.
[11] R. Castaño-Rosa, R. Barrella, C. Sánchez-Guevara, R. Barbosa, I. Kyprianou, E. Paschalidou, et al., Cooling degree models and future energy demand in the residential sector. A seven-country case study, Sustainability 13 (2021) 2987, https://doi.org/10.3390/su13052987.
[12] C. Zhang, O.B. Kazanci, R. Levinson, P. Heiselberg, B.W. Olesen, G. Chiesa, et al., Resilient cooling strategies – a critical review and qualitative assessment, Energy Build. 251 (2021) 111312, https://doi.org/10.1016/j.enbuild.2021.111312.
[13] E. Elnagar, A. Zeoli, R. Rahif, S. Attia, V. Lemort, A qualitative assessment of integrated active cooling systems: a review with a focus on system flexibility and climate resilience, Renew. Sustain. Energy Rev. 175 (2023) 113179, https://doi.org/10.1016/j.rser.2023.113179.
[14] IEA- International Energy Agency, The Future of Cooling- Opportunities for Energy Efficient Air Conditioning, 2018.
[15] S. Pezzutto, G. Quaglini, P. Riviere, L. Kranzl, A. Novelli, A. Zambito, et al., Screening of cooling technologies in Europe: alternatives to vapour compression and possible market developments, Sustainability 14 (2022) 2971, https://doi.org/10.3390/su14052971.
[16] Y. Song, K.S. Darani, A.I. Khdair, G. Abu-Rumman, R. Kalbasi, A review on conventional passive cooling methods applicable to arid and warm climates considering economic cost and efficiency analysis in resource-based cities, Energy Rep. 7 (2021) 2784–2820, https://doi.org/10.1016/j.egyr.2021.04.056.
[17] E. Elnagar, B. Köhler, Reduction of the energy demand with passive approaches in multifamily nearly zero-energy buildings under different climate conditions, Front. Energy Res. 8 (2020), https://doi.org/10.3389/fenrg.2020.545272.
[18] A. Moret Rodrigues, M. Santos, M.G. Gomes, R. Duarte, Impact of natural ventilation on the thermal and energy performance of buildings in a mediterranean climate, Buildings 9 (2019) 123, https://doi.org/10.3390/buildings9050123.
[19] S. Attia, C. Gobin, Climate change effects on Belgian households: a case study of a nearly zero energy building, Energies 13 (2020) 5357, https://doi.org/10.3390/en13205357.
[20] E. Elnagar, A. Zeoli, V. Lemort, Performance evaluation of passive cooling in a MultiZone apartment building based on natural ventilation, in: Proceedings of CLIMA 2022: 14th REHVA HVAC, World Congress, Rotterdam, 2022.
[21] K. Bamdad, S. Matour, N. Izadyar, T. Law, Introducing extended natural ventilation index for buildings under the present and future changing climates, Build. Environ. 226 (2022) 109688, https://doi.org/10.1016/j.buildenv.2022.109688.
[22] X. Xie, Z. Luo, S. Grimmond, T. Sun, Impact of building density on natural ventilation potential and cooling energy saving across Chinese climate zones, Build. Environ. 244 (2023) 110621, https://doi.org/10.1016/j.buildenv.2023.110621.
[23] Z. Tong, Y. Chen, A. Malkawi, Z. Liu, R.B. Freeman, Energy saving potential of natural ventilation in China: the impact of ambient air pollution, Appl. Energy 179 (2016) 660–668, https://doi.org/10.1016/j.apenergy.2016.07.019.
[24] R. Rahif, A. Norouziasas, E. Elnagar, S. Doutreloup, S.M. Pourkiaei, D. Amaripadath, et al., Impact of climate change on nearly zero-energy dwelling in temperate climate: time-integrated discomfort, HVAC energy performance, and GHG emissions, Build. Environ. 223 (2022) 109397, https://doi.org/10.1016/j.buildenv.2022.109397.
[25] E. Elnagar, S. Gendebien, E. Georges, U. Berardi, S. Doutreloup, V. Lemort, Framework to assess climate change impact on heating and cooling energy demands in building stock: a case study of Belgium in 2050 and 2100, Energy Build. 298 (2023) 113547, https://doi.org/10.1016/j.enbuild.2023.113547.
[26] R. Rahif, M. Hamdy, S. Homaei, C. Zhang, P. Holzer, S. Attia, Simulation-based framework to evaluate resistivity of cooling strategies in buildings against overheating impact of climate change, Build. Environ. 208 (2022) 108599, https://doi.org/10.1016/j.buildenv.2021.108599.
[27] H. Hooyberghs, S. Verbeke, D. Lauwaet, H. Costa, G. Floater, K. De Ridder, Influence of climate change on summer cooling costs and heat stress in urban office buildings, Climatic Change 144 (2017) 721–735, https://doi.org/10.1007/s10584-017-2058-1.
[28] B. Bandyopadhyay, M. Banerjee, Decarbonization of cooling of buildings, Solar Compass 2 (2022) 100025, https://doi.org/10.1016/j.solcom.2022.100025.
[29] H. Yan, F. Shi, Z. Sun, G. Yuan, M. Wang, M. Dong, Thermal adaptation of different set point temperature modes and energy saving potential in split air-conditioned

office buildings during summer, Build. Environ. 225 (2022) 109565, https://doi.org/10.1016/j.buildenv.2022.109565.
[30] H. Yan, Z. Sun, F. Shi, G. Yuan, M. Dong, M. Wang, Thermal response and thermal comfort evaluation of the split air conditioned residential buildings, Build. Environ. 221 (2022) 109326, https://doi.org/10.1016/j.buildenv.2022.109326.
[31] A. Roetzel, A. Tsangrassoulis, Impact of climate change on comfort and energy performance in offices, Build. Environ. 57 (2012) 349–361, https://doi.org/10.1016/j.buildenv.2012.06.002.
[32] T. Berger, C. Amann, H. Formayer, A. Korjenic, B. Pospischal, C. Neururer, et al., Impacts of climate change upon cooling and heating energy demand of office buildings in Vienna, Austria, Energy Build. 80 (2014) 517–530, https://doi.org/10.1016/j.enbuild.2014.03.084.
[33] K. Jylhä, J. Jokisalo, K. Ruosteenoja, K. Pilli-Sihvola, T. Kalamees, T. Seitola, et al., Energy demand for the heating and cooling of residential houses in Finland in a changing climate, Energy Build. 99 (2015) 104–116, https://doi.org/10.1016/j.enbuild.2015.04.001.
[34] T. van Hooff, B. Blocken, H.J.P. Timmermans, J.L.M. Hensen, Analysis of the predicted effect of passive climate adaptation measures on energy demand for cooling and heating in a residential building 94 (2016) 811–820, https://doi.org/10.1016/j.energy.2015.11.036.
[35] V. Pérez-Andreu, C. Aparicio-Fernández, A. Martínez-Ibernón, J.-L. Vivancos, Impact of climate change on heating and cooling energy demand in a residential building in a Mediterranean climate 165 (2018) 63–74, https://doi.org/10.1016/j.energy.2018.09.015.
[36] A. Moazami, V.M. Nik, S. Carlucci, S. Geving, Impacts of future weather data typology on building energy performance – investigating long-term patterns of climate change and extreme weather conditions, Appl. Energy 238 (2019) 696–720, https://doi.org/10.1016/j.apenergy.2019.01.085.
[37] R.F. De Masi, A. Gigante, S. Ruggiero, G.P. Vanoli, Impact of weather data and climate change projections in the refurbishment design of residential buildings in cooling dominated climate, Appl. Energy 303 (2021) 117584, https://doi.org/10.1016/j.apenergy.2021.117584.
[38] M. Olonscheck, A. Holsten, J.P. Kropp, Heating and cooling energy demand and related emissions of the German residential building stock under climate change, Energy Pol. 39 (2011) 4795–4806, https://doi.org/10.1016/j.enpol.2011.06.041.
[39] V.M. Nik, Kalagasidis A. Sasic, Impact study of the climate change on the energy performance of the building stock in Stockholm considering four climate uncertainties, Build. Environ. 60 (2013) 291–304, https://doi.org/10.1016/j.buildenv.2012.11.005.
[40] M. Hamdy, S. Carlucci, P.-J. Hoes, J.L.M. Hensen, The impact of climate change on the overheating risk in dwellings—a Dutch case study, Build. Environ. 122 (2017) 307–323, https://doi.org/10.1016/j.buildenv.2017.06.031.
[41] M.A.D. Larsen, S. Petrović, A.M. Radoszynski, R. McKenna, O. Balyk, Climate change impacts on trends and extremes in future heating and cooling demands over Europe, Energy Build. 226 (2020) 110397, https://doi.org/10.1016/j.enbuild.2020.110397.
[42] E. Georges, S. Gendebien, B. Dechesne, S. Bertagnolio, V. Lemort, Impact of the integration of various heating technologies on the energy load profiles of the Belgian residential building stock. Proceedings of IRES 2013 Conference, 2013.
[43] E. Georges, S. Gendebien, S. Bertagnolio, V. Lemort, Modeling and simulation of the domestic energy use in Belgium following a bottom-up approach. Proceedings of the CLIMA 2013 11th REHVA World Congress & 8th International Conference on IAQVEC, 2013.
[44] W. Cyx, N. Renders, M. Van Holm, S. Verbeke, IEE TABULA-Typology Approach for Building Stock Energy Assessment, 2011. Mol, Belgium.
[45] D. Vanneste, I. Thomas, L. Goossens, Enquête socio-économique 2001 - Monographie «Le logement en Belgique». SPF Economie, Direction generale Statistique et Information Economique (DGSIE), Politique scientifique fédérale, 2007.
[46] H. Hens, G. Verbeeck, B. Verdonck, Impact of energy efficiency measures on the CO2 emissions in the residential sector, a large scale analysis, Energy Build. 33 (2001) 275–281, https://doi.org/10.1016/S0378-7788(00)00092-X.
[47] S. Gendebien, E. Georges, S. Bertagnolio, V. Lemort, Methodology to characterize a residential building stock using a bottom-up approach: a case study applied to Belgium, International Journal of Sustainable Energy Planning and Management (2015) 71–88, https://doi.org/10.5278/IJSEPM.2014.4.7.
[48] EUROSTAT. Statistics Belgium, EUROPEAN STATISTICAL RECOVERY DASHBOARD, 2011. https://statbel.fgov.be/en.
[49] E. Van Hecke, H. Jean-Marie, J.-M. Decroly, B. Mérenne-Schoumaker, Noyaux d'habitat et Régions urbaines dans une Belgique urbanisée, 2009.
[50] Department of Energy and Sustainable Buildings - Office for Sustainable Buildings, WALLOON LONG-TERM BUILDING RENOVATION STRATEGY, 2021.
[51] T. Boermans, K. Bettgenhäuser, M. Offermann, S. Schimschar, Renovation Tracks for Europe up to 2050, 2012.
[52] R. Verhoeven, Pathways to World-Class Energy Efficiency in Belgium, McKinsey & Company-, Belgium, 2009, 2009.
[53] European Union, Directive 2010/31/EU of the European Parliament and of the Council of 19 May 2010 on the Energy Performance of Buildings, 2010.
[54] E. Elnagar, C. Davila, V. Lemort, Impact of integration of electric and gas heat pumps on the final energy consumption of Belgian residential building stock. CLIMA 2022 Conference, 2022, https://doi.org/10.34641/clima.2022.102.
[55] S. Doutreloup, X. Fettweis, R. Rahif, E. Elnagar, M.S. Pourkiaei, D. Amaripadath, et al., Historical and future weather data for dynamic building simulations in Belgium using the regional climate model MAR: typical and extreme meteorological year and heatwaves, Earth Syst. Sci. Data 14 (2022) 3039–3051, https://doi.org/10.5194/essd-14-3039-2022.
[56] S. Doutreloup, C. Wyard, C. Amory, C. Kittel, M. Erpicum, X. Fettweis, Sensitivity to convective schemes on precipitation simulated by the regional climate model MAR over Belgium (1987–2017), Atmosphere 10 (2019) 34, https://doi.org/10.3390/atmos10010034.
[57] C. Wyard, C. Scholzen, S. Doutreloup, É. Hallot, X. Fettweis, Future evolution of the hydroclimatic conditions favouring floods in the south-east of Belgium by 2100 using a regional climate model, Int. J. Climatol. 41 (2021) 647–662, https://doi.org/10.1002/joc.6642.
[58] X. Fettweis, C. Wyard, S. Doutreloup, A. Belleflamme, Noël 2010 en Belgique : neige en Flandre et pluie en Haute-Ardenne. https://popups.uliege.be/0770-7576n.d. (Accessed 20 January 2022). https://popups.uliege.be/0770-7576/index.php?id=4568&format=print.
[59] S. Doutreloup, B. Bois, B. Pohl, S. Zito, Y. Richard, Climatic comparison between Belgium, Champagne, Alsace, Jura and Bourgogne for wine production using the regional model MAR, OENO One 56 (2022) 1–17, https://doi.org/10.20870/oeno-one.2022.56.3.5356.
[60] H. Hersbach, B. Bell, P. Berrisford, S. Hirahara, A. Horányi, J. Muñoz-Sabater, et al., The ERA5 global reanalysis, Q. J. R. Meteorol. Soc. 146 (2020) 1999–2049, https://doi.org/10.1002/qj.3803.
[61] T. Wu, R. Yu, Y. Lu, W. Jie, Y. Fang, J. Zhang, et al., BCC-CSM2-HR: a high-resolution version of the Beijing climate center climate system model, Climate and Earth system modeling (2020), https://doi.org/10.5194/gmd-2020-284.
[62] K. Riahi, D.P. van Vuuren, E. Kriegler, J. Edmonds, B.C. O'Neill, S. Fujimori, et al., The Shared Socioeconomic Pathways and their energy, land use, and greenhouse gas emissions implications: an overview, Global Environ. Change 42 (2017) 153–168, https://doi.org/10.1016/j.gloenvcha.2016.05.009.
[63] J.M. Finkelstein, R.E. Schafer, Improved goodness-of-fit tests, Biometrika 58 (1971) 641–645, https://doi.org/10.1093/biomet/58.3.641.
[64] D. Ramon, K. Allacker, N.P.M. van Lipzig, F. De Troyer, H. Wouters, Future weather data for dynamic building energy simulations: overview of available data and presentation of newly derived data for Belgium, in: E. Motoasca, A.K. Agarwal, H. Breesch (Eds.), Energy Sustainability in Built and Urban Environments, Springer Singapore, Singapore, 2019, pp. 111–138, https://doi.org/10.1007/978-981-13-3284-5_6.
[65] International Organization for Standardization, European Standard: ISO 15927-4 Hygrothermal Performance of Buildings — Calculation and Presentation of Climatic Data — Part 4: Hourly Data for Assessing the Annual Energy Use for Heating and Cooling, 2005.
[66] Royal Meteorological Institute of Belgium, Rapport climatique 2020 de l'information aux services climatiques, 2020. Brussels Belgium.
[67] FPS Public Health, Food Chain Safety and Environment of Belgium. Hittegolf en Ozonpiekenplan, 2008.
[68] G. Ouzeau, J.-M. Soubeyroux, M. Schneider, R. Vautard, S. Planton, Heat waves analysis over France in present and future climate: application of a new method on the EURO-CORDEX ensemble, Climate Services 4 (2016) 1–12, https://doi.org/10.1016/j.cliser.2016.09.002.
[69] C. Zhang, O.B. Kazanci, S. Attia, R. Levinson, S.H. Lee, P. Holzer, et al., IEA EBC Annex 80 - dynamic simulation guideline for the performance testing of resilient cooling strategies: version 2. Aalborg: Department of the Built Environment, Aalborg University, 2023.
[70] R. Rahif, D. Amaripadath, S. Attia, Review on time-integrated overheating evaluation methods for residential buildings in temperate climates of Europe, Energy Build. 252 (2021) 111463, https://doi.org/10.1016/j.enbuild.2021.111463.
[71] International Organization for Standardization, ISO 17772-1:2017: Energy Performance of Buildings — Indoor Environmental Quality — Part 1: Indoor Environmental Input Parameters for the Design and Assessment of Energy Performance of Buildings, 2017.
[72] European Committee for Standardization, CEN, EN 16798-1: energy performance of buildings - ventilation for buildings - indoor environmental input parameters for design and assessment of energy performance of buildings addressing indoor air quality. Thermal Environment, Lighting and Acoustics, 2019. Brussels, Belgium.
[73] B. Koffi, A. Cerutti, M. Duerr, A. Iancu, A. Kona, G. Janssens-Maenhout, Covenant of Mayors for Climate and Energy: Default Emission Factors for Local Emission Inventories, JRC Publications Repository, 2017, https://doi.org/10.2760/290197.
[74] International Energy Agency (IEA). Data & Statistics. IEA n.d. https://www.iea.org/data-and-statistics/data-browser (accessed March 31, 2022).
[75] ASHRAE, Handbook—Fundamentals. American Society of Heating, Refrigeration, and Air-Conditioning Engineers, 2021.
[76] International Organization for Standardization. ISO 15927-2:2009 - Hygrothermal Performance of Buildings — Calculation and Presentation of Climatic Data — Part 2: Hourly Data for Design Cooling Load n.d.
[77] M. Luo, R. de Dear, W. Ji, C. Bin, B. Lin, Q. Ouyang, et al., The dynamics of thermal comfort expectations: the problem, challenge and impication, Build. Environ. 95 (2016) 322–329, https://doi.org/10.1016/j.buildenv.2015.07.015.
[78] W. Luan, X. Li, Rapid urbanization and its driving mechanism in the Pan-Third Pole region, Sci. Total Environ. 750 (2021) 141270, https://doi.org/10.1016/j.scitotenv.2020.141270.
[79] Belgian Science Policy. PROJECT LEHR: LOW ENERGY HOUSING RETROFIT n.d. http://www.lehr.be/(accessed August 13, 2023).